Universidade do Minho
Escola de Ciências

Patrícia Alexandra Gomes Cerqueira

Development of PEGylated nanoparticles for delivery of methotrexate derivatives

Outubro de 2018

UMinho | 2018 Patrícia Cerqueira **Development of PEGylated nanoparticles for delivery of methotrexate derivatives**

Universidade do Minho
Escola de Ciências

Patrícia Alexandra Gomes Cerqueira

Development of PEGylated nanoparticles for delivery of methotrexate derivatives

Tese de Mestrado
Mestrado em Bioquímica Aplicada (Área de especialização em Biotecnologia)

Trabalho efetuado sob a orientação da
Doutora Ana Isabel Sá Loureiro

e do
Professor Doutor João Carlos Ramos Nunes Marcos

Outubro de 2018

DECLARAÇÃO

Nome: Patrícia Alexandra Gomes Cerqueira

Endereço eletrónico: patricia.a.g.cerqueira@gmail.com Telefone: 962346317

Cartão do Cidadão: 14893733

Título da dissertação: Development of PEGylated nanoparticles for delivery of methotrexate derivatives

Orientadores:

Doutora Ana Isabel Sá Loureiro

Professor Doutor João Carlos Ramos Nunes Marcos

Ano de conclusão: 2018

Mestrado em Bioquímica Aplicada, área de especialização em Biotecnologia

Universidade do Minho, 29 de Outubro de 2018

To my dear father

Ao meu querido pai

Acknowledgements/ Agradecimentos

A realização desta tese contou com importantes apoios e incentivos, sendo estes as principais razões que tornaram este trabalho possível e aos quais estarei eternamente grata.

Gostaria antes de mais agradecer aos meus orientadores, em especial à **Dr.ª Ana Loureiro** pelo excelente trabalho como orientadora, pelo total apoio, incentivo, opiniões, críticas, disponibilidade assim como pela total colaboração no solucionar de problemas e esclarecimento de dúvidas durante a realização do presente trabalho. Obrigada pela paciência, ajuda e por me ter permitido adquirir competências que irão ser essenciais no futuro.

Gostaria também de agradecer a oportunidade de ter pertencido ao grupo de investigação **BBRG**. Agradeço ao **Professor Artur Cavaco Paulo** pela oportunidade de realizar este trabalho no seu grupo de investigação e a todos os investigadores do grupo pela ajuda e companheirismo, em especial à **Jennifer** e à **Diana**. Vocês foram sempre impecáveis, estando sempre prontas a ajudar quando necessário. Obrigada **Jennifer** pela paciência, pela boa disposição e pelos conhecimentos químicos, que foram uma grande ajuda! Obrigada **Diana**, és uma pessoa com um coração enorme e bondoso, por isso agradeço todos os ensinamentos e apoio, mesmo nos mais ínfimos pormenores.

Agradeço também o auxílio por parte da minha colega de projeto e também grande amiga, **Sofia**, por todos os conselhos e informações fornecidas e também pelo companheirismo e apoio demonstrados. Foste impecável e um grande suporte mental! Obrigada por sempre me incentivares e ajudares! A tua amizade foi uma das melhores coisas que me aconteceu neste mestrado.

Para além desta grande ajuda fornecida, tenho também de agradecer imenso à minha irmã do coração, **Andreia**, por sempre me ouvir e apoiar nos bons e maus momentos. Sempre foste, és e serás um dos pilares da minha vida. Sem ti, nunca chegaria onde cheguei nem seria quem sou hoje! Obrigada pela amizade e paciência!

Gostava de agradecer aos meus amigos, que sempre estiveram ao meu lado e sempre me apoiaram. A vossa amizade é muito importante para mim!

Também queria agradecer bastante à minha família, em especial aos meus **pais**, **irmã**, **avós maternos** e ao meu **tio** pois sem o seu total apoio, força e compreensão não teria conseguido aguentar e ultrapassar esta época complicada e realizar este trabalho. Vocês são essenciais na minha vida!

Quero fazer um especial agradecimento à minha querida mãe, **Teresa**, uma guerreira que eu admiro imenso pois apesar de todos os obstáculos e adversidades, sempre perseveraste e sempre estiveste lá por nós e para nós. Obrigada por fazeres de mim quem sou hoje, pelos conselhos, pela dedicação, amor, incentivo, apoio e por sempre estares ao meu lado.

Também gostaria de agradecer imenso ao meu querido pai, **Fernando**, que apesar de não estar ao meu lado estará para sempre no meu coração. Obrigada por me teres mostrado que lutando tudo é possível. Obrigada por me ensinares a não desistir e por me mostrares que a força que existe dentro de nós é ilimitada! Nunca me vou esquecer do teu sorriso e dos teus olhos a brilhar sempre que falavas de nós e do orgulho que demostravas em nós.

Muito obrigada a todos vocês!

Abstract – DEVELOPMENT OF PEGYLATED NANOPARTICLES FOR DELIVERY OF METHOTREXATE DERIVATIVES

Cancer is one of the most devastating and life-threatening diseases, and conventional chemotherapeutic agents, such as methotrexate (MTX), present several limitations and adverse effects. The use of nanoparticles (NPs) enables an efficient alternative to conventional therapy as they can overcome these limitations. NPs may be engineered to have a prolonged circulation time, enhanced cellular uptake and targeting abilities. One widely used targeting approach is the development of NPs containing folic acid (FA) at the surface. Folate receptor (FR) is overexpressed in tumor cells and is not expressed or is present at low levels in normal cells. In this way, FA-tagged NPs allow a specific delivery of the drug. Although several types of NPs have been developed as drug delivery systems (DDS), this work focused on the polymeric micelles and liposomes. Thus, the main aim of this project was the development of PEGylated micelles and liposomes with suitable characteristics for intravenous (IV) administration and with the ability to delivery hydrophobic MTX derivatives to a target cell population. First of all, micelles and liposomes production methods were optimized. For the micelles production were tested two different methods, auxiliary solvent method and sonication, and the liposomes were produced using ethanol injection method. The full characterization of the developed NPs was performed, including the analysis of their physicochemical properties, stability, drug encapsulation efficiency (EE) and biological effect. The use of the auxiliary solvent method with evaporation at 30 °C, a polyoxyethanyl-α-tocopheryl sebacate (PTS) concentration of 15 mg/mL and a PTS/MTX diethylated (MTX-OEt) mass ratio of 8:1 resulted in monodisperse micelles with small size. These PEGylated micelles revealed the expected biological effect against cancer cells (Caco-2 cells). In the case of liposomes, the ideal formulation was reached using a lipid concentration of 9 mM, water as aqueous phase, a MTX-dimethyldioctadecylammonium bromide (MTX-DODAB) concentration of 2.91 mg/mL and an initial water/ethanol volume of 6/6 mL. The obtained liposomes also showed suitable characteristics including a monodisperse population of small and neutral particles and demonstrated a significant cytotoxicity against cancer cells, similar to free MTX.

In sum, the developed PEGylated micelles and liposomes loaded with hydrophobic MTX derivatives demonstrated to be promising DDS for cancer therapy.

Resumo – DESENVOLVIMENTO DE NANOPARTÍCULAS PEGUILADAS PARA A ENTREGA DE DERIVADOS DE METOTREXATO

O cancro é uma das doenças mais devastadoras e fatais, e os agentes quimioterápicos convencionais, como o metotrexato (MTX), apresentam várias limitações e efeitos adversos. O uso de nanopartículas (NPs) possibilita uma alternativa eficiente à terapia convencional, pois estas podem superar essas limitações. As NPs podem ser projetadas para ter um tempo de circulação prolongado, melhor captação celular e habilidades de direcionamento. Uma abordagem de direcionamento amplamente utilizada é o desenvolvimento de NPs contendo ácido fólico (FA, do inglês *folic acid*) à superfície. O recetor de folato (FR, do inglês *folate receptor*) é sobre-expresso em células tumorais e não é expresso ou está presente em níveis baixos em células normais. Deste modo, as NPs com FA permitem uma entrega específica do fármaco. Embora vários tipos de NPs tenham sido desenvolvidos como sistemas de entrega de fármacos (DDS, do inglês *drug delivery systems*), este trabalho focou-se nas micelas poliméricas e nos lipossomas. Assim, o principal objetivo deste projeto foi o desenvolvimento de micelas e lipossomas PEGuilados com características adequadas para administração intravenosa (IV) e com a capacidade de entregar derivados hidrofóbicos de MTX a uma população de células alvo. Primeiramente, os métodos de produção de micelas e lipossomas foram otimizados. Para a produção de micelas foram testados dois métodos diferentes, o método do solvente auxiliar e sonicação, e os lipossomas foram produzidos pelo método de injeção etanólica. A caracterização completa das NPs desenvolvidas foi realizada, incluindo a análise das suas propriedades físico-químicas, estabilidade, eficiência de encapsulação do fármaco (EE) e efeito biológico. O uso do método do solvente auxiliar com evaporação a 30 °C, uma concentração de sebacato de polioxietanil-α-tocoferil (PTS) de 15 mg/mL e uma relação mássica de PTS/MTX dietilado (MTX-OEt) de 8:1 originou micelas monodispersas e com tamanho pequeno. Estas micelas PEGuiladas revelaram o efeito biológico esperado contra células de cancro (células Caco-2). No caso dos lipossomas, a formulação ideal foi alcançada utilizando uma concentração lipídica de 9 mM, água como fase aquosa, uma concentração de MTX-brometo de dimetildioctadecilamónio (MTX-DODAB) de 2.91 mg/mL e um volume inicial de água/etanol de 6/6 mL. Os lipossomas obtidos também apresentaram características adequadas, incluindo uma população monodispersa de partículas pequenas e neutras que demonstraram uma citotoxicidade significativa contra células de cancro, semelhante ao MTX livre.

Em suma, as micelas e os lipossomas PEGuilados desenvolvidos, carregados com derivados hidrofóbicos de MTX, demostraram ser DDS promissores para a terapia do cancro.

Table of Contents

Figures Index

Tables Index

Equations Index

Abbreviations and Acronyms Index

0-9

^{1}H NMR, NMR	Proton nuclear magnetic resonance

A

ATCC	American type culture collection

C

CMC	Critical micelle concentration

D

DDS	Drug delivery systems
DHB	2,5-dihydroxybenzoic acid
DLS	Dynamic light scattering
DMEM	Dulbecco's modified eagle's medium
DMSO	Dimethylsulfoxide
DMSO-d_6	Deuterated dimethylsulfoxide
DNA	Deoxyribonucleic acid
DODAB	Dimethyldioctadecylammonium bromide
DOPE	1,2-ioleoyl-sn-glycero-3-phosphoethanolamine
DSPE	1,2-distearoyl-sn-glycero-3-phosphoethanolamine
DSPE-mPEG 2000	1,2-distearoyl-sn-glycero-3-phosphoethanolamine-*N*-[carboxy(polyethylene glycol)-2000]

E

EE	Encapsulation efficiency
EG	Ethylene glycol
EPR	Enhanced permeability and retention

F

FA	Folic acid
FBS	Fetal bovine serum
FDA	Food and drug administration
FH_2	Dihydrofolate
FH_4	Tetrahydrofolate
FR	Folate receptor
FTIR	Fourier-transform infrared

H

HPLC	High-performance liquid chromatography

I

IV	Intravenous

K

KR2i TFF	KrosFlo® research 2i tangential flow filtration

M

MALDI-TOF	Matrix-assisted laser desorption/ionization time-of-flight
MDR	Multidrug resistance
mPES	Modified polyethersulfone
MPS	Mononuclear phagocyte system
MTS	3-(4,5-dimethylthiazol-2-yl)-5-(3-carboxymethoxyphenyl)-2-(4-sulfophenyl)-2*H*-tetrazolium
MTX	Methotrexate
MTX-Na	Methotrexate disodium salt
MTX-OEt	Methotrexate diethylated
MW	Molecular weight
$MW_{average}$	Average molecular weight

MWCO	Molecular weight cut-off

N

NPs	Nanoparticles
NTA	Nanoparticle tracking analysis

P

PBS	Phosphate buffered saline
PCS	Photon correlation spectroscopy
PdI	Polydispersity index
PEG	Poly(ethylene glycol)
PES	Polyethersulfone
PTS	Polyoxyethanyl-α-tocopheryl sebacate

R

RES	Reticuloendothelial system
RNA	Ribonucleic acid
RT	Room temperature

S

SD	Standard deviation

T

TEA	Triethylamine
TMP	Thymidylate

CHAPTER I

Objectives and Outline

Chapter I – OBJECTIVES AND OUTLINE

1. OBJECTIVES OF THE WORK

The aim of this work is the development of nanoparticles (NPs) with suitable properties to provide an efficient and novel treatment option, mainly for cancer therapy. These NPs should present adequate characteristics for intravenous (IV) administration such as small size and stealth properties, they should also be able to entrap hydrophobic drugs successfully and, if possible, should present a targeting agent at the surface (for example: folic acid (FA)) for a specific delivery of the pharmacological compound to a target cell population. All these characteristics are very important for overcoming the side effects that are greatly associated with conventional therapies and also for enhancing the drug therapeutic effect.

In this way, the main objectives of this work are: the production of small and PEGylated NPs (micelles and liposomes); the encapsulation of hydrophobic methotrexate (MTX) derivatives (MTX diethylated (MTX-OEt) and MTX-dimethyldioctadecylammonium bromide (MTX-DODAB)) in these developed NPs and the *in vitro* evaluation of their ability to carry and deliver these MTX derivatives.

2. OUTLINE OF THE THESIS

In agreement with the aims of this master thesis, this document is divided into 5 chapters. The contents of each chapter are described below.

The first and current chapter contains the main purposes of this work, as well as an introduction to the thesis outline and format.

The second chapter consists in the state of art of this thesis theme, in which it is resumed all the information needed for a full understanding of the work presented in the next chapters.

Chapter three and four describe all the materials and methods used in this work, as well as the results obtained, its discussion and main conclusions of the research work performed regarding micelles and liposomes, respectively.

This master thesis ends with chapter five, which presents the final remarks of the developed work and the future perspectives for this research work.

CHAPTER II
General Introduction

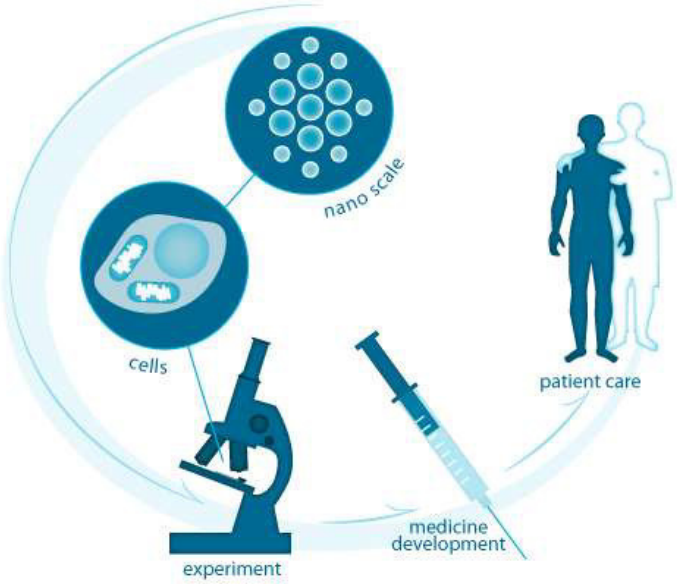

Chapter II – GENERAL INTRODUCTION

1. NANOTECHNOLOGY, NANOMEDICINE AND NANODEVICES

Nanotechnology is a multidisciplinary field in which several areas of knowledge, such as engineering, biology, physics and chemistry, are linked to develop and produce materials at the atomic and molecular scale [1-3]. This field involves the design, synthesis, characterization and application of materials, devices or systems at the nanometer scale with the objective to control material behaviour and add novel properties and functions [2, 4]. Nanotechnology has applications in several different fields such as medicine, chemistry, cosmetics, agriculture and food industry, bioinformatics, communication and construction [5]. In the last decades, the breakthroughs in nanotechnology allowed the emergence of several new possibilities in medical sciences and numerous platforms are being investigated and developed in order to attain more effective and safer therapeutics [2, 6]. Nanomedicine, one of the most important fields of nanotechnology, focus in a highly specific medical intervention at a molecular scale for diagnosis, prevention and treatment of diseases [7]. As it can be seen in figure 1, there are several fields of medicine in which nanotechnology intervention is promising [8].

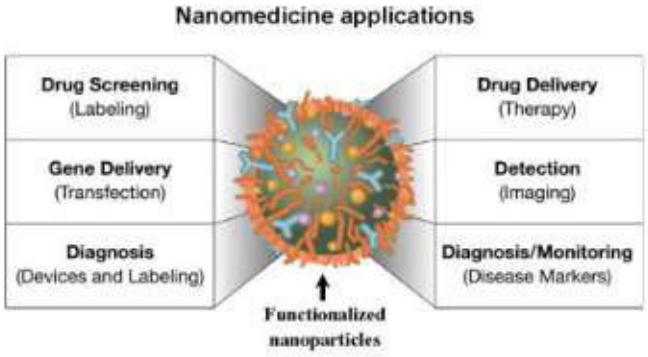

Figure 1 | Applications and research targets of nanomedicine [From Liu *et al.*, 2007 [8]].

Recently, there has been an enormous increase in the use of nanomedicine formulations which show a great potential, enabling more effective and less toxic diagnostic and therapeutic interventions [9]. The main objective of nanomedicine has been the development of nanomaterials with specific applications in order to offer a suitable means to deliver small molecular weight (MW) drugs and provide a mechanism for local or site specific targeted delivery of macromolecules [10]. In the last years, nanomedicine has focused on the development of drug delivery systems (DDS)

for the treatment of diseases [11], allowing the emergence of several novel nanomaterials [11-13]. These nanomaterials offer multiple desirable attributes and can overcome the problems of conventional therapy, improving drug delivery efficiency [11-13]. A DDS is defined as a formulation or a device that enables the introduction of a therapeutic compound in the body using various routes of administration, improving the drug's efficacy and safety by controlling the rate, time and place of release [10, 14]. These systems can overcome some obstacles in drug delivery, such as the targeting of diverse cell types, drug resistance problems and the biological barriers [15].

Drugs can be administrated by numerous routes, such as enteral (oral, sublingual and rectum administration), parenteral (IV, intramuscular, subcutaneous and inhalation administration) or topical (skin and mucosal membranes) [16]. The route of the drug comprises several steps: the administration of the drug, its distribution through the body, the passage through the different pathways and barriers and the transport of the drugs to their target organs [17, 18]. The passage of the drug molecules across the several physiological barriers is one of the most important obstacles to surpass in drug delivery [19]. Conventional drugs can adversely affect other cells and tissues, reducing the effectiveness of the treatment, and they are often cleared too quickly from the bloodstream by the kidneys or through immune recognition [18]. Additionally, conventional drugs may be unstable and degrade quickly, may have a very poor solubility in aqueous solution or may exhibit toxicity as well as unsuitable interactions with other chemical species [18, 20]. Therefore, some conventional drugs cannot be delivered using conventional release methods [20]. In order to overcome all these problems, NPs have been a premier choice as DDS to carry the drug in a controlled manner and to improve the pharmacological and therapeutic properties of the drugs [17, 19, 21].

In the development of NPs there are four essential prerequisites that need to be followed: drug retention; immune system escape, extending the circulation time; targeting to the diseased site, avoiding most healthy organs; and release of the drug [22].

1.1. Design of suitable nanoparticles for intravenous administration

The most reliable route of entry for NPs is the IV route because it's the fastest and easiest administration method that allows a quick and complete distribution across the body via the systemic circulation [23, 24]. After IV administration, NPs have to overcome multiple obstacles: the clearance by the mononuclear phagocyte system (MPS), also referred as reticuloendothelial

system (RES); the immune barrier including the reaction of the immune system, activation of the complement cascade and allergic responses to foreign materials; the fast renal elimination by glomerular filtration and the blood vessel wall, particularly the endothelial cell lining and basement membranes that prevent direct access to organs and tissues at the capillary level [23]. The MPS consists in a system of phagocytic cells, predominantly resident macrophages in the spleen, lymph nodes and liver [25]. This system is responsible for the body's defence and filtration mechanisms, removing old or irregular red and white blood cells, as well as opsonized components and large foreign objects [26, 27]. MPS seize the NPs by opsonization, which is a process that involves the adsorption of plasma proteins [25]. After opsonization the NPs are recognized by specific receptors on the phagocytes' surface and internalized, resulting in the clearance of the drug carriers from the body [25]. This process is a major obstacle to the drug delivery to the target site of therapeutic action [28].

The biodistribution of NPs administered intravenously to the target site is strongly dependent on their physicochemical properties, such as size and surface characteristics [29]. The shape of the NPs is also an important characteristic because it affects NPs behaviour and motion in blood flow, membrane adhesion strength, cell uptake pathways and efficacy [23, 30]. However, this property will not be studied into further detail because the majority of NPs used for drug delivery tend to be spherical [30]. In order to overcome the main biological barriers and to prevent early clearance of NPs, the size and surface characteristics can be coordinated providing the adequate features to NPs [31-33].

The size is an important parameter in the design of long-circulating NPs and a key factor in the process of particle internalization [26, 30]. This parameter determines the *in vivo* distribution, toxicity and targeting ability of NPs and can also influence drug loading, drug release and *in vitro* and *in vivo* stability [26, 30]. Moreover, this physicochemical property can affect the efficiency and pathway of cellular uptake of the NPs [34]. Particle size determines if the NPs are opsonized and rapidly cleared by the MPS or if the NPs are cleared by glomerular filtration [35]. Fast clearance of the particles by glomerular filtration is observed below 5.5 nm [23]. On the other hand, NPs with a diameter higher than 200 nm typically exhibit rapid opsonization and uptake by the MPS, being sequestered in liver and spleen [36]. Considering that opsonization leads to aggregation and rapid clearance from the bloodstream, it's demonstrated that smaller particles possess a slower blood clearance than the larger NPs, improving nanoparticle blood residence and accumulation in

specific tissues for the treatment of disease [37]. Therefore, an optimal size range for NPs is between 10 and 100 nm, avoiding the clearance by the MPS or the glomerular filtration [26, 38].

The surface characteristics of NPs represent another essential parameter in the determination of their drug loading efficiency, release profile, circulation half-life, targeting and clearance from the body [30]. The surface properties of a particle can also affect its interactions with molecules, cells or physiological systems [26] as well as the efficiency of extravasation and retention [30]. The main physicochemical characteristics of the NPs' surface to consider are the surface charge, functional groups and hydrophobicity [34, 37].

The surface charge of NPs, which is determined by the zeta-potential [39], determines the adsorption of plasma proteins, leading to their recognition by macrophages, followed by phagocytosis and elimination [34]. Positively charged particles tend to form aggregates after neutralisation of their net charge, showing increased recognition by the immune system [36, 40]. Moreover, an increased phagocytosis, higher rate of cell uptake, higher nonspecific internalization rate and short blood circulation half-life happens for positively charged NPs because of their better interaction with the anionic cell membrane [34, 37, 40]. On the other hand, negatively charged NPs show a low phagocytic uptake, thereby contributing to the increase of blood circulation time [34]. As the surface charge becomes larger (either positive or negative), macrophage uptake is increased and can lead to greater clearance by MPS [40]. Neutral NPs are the ideal ones because they are associated with lower opsonization rates than charged NPs, reducing their clearance from the blood circulation [37, 41]. The presence of functional groups also has an important role on the NPs' behaviour because it is known that particles containing a primary amine at the surface are more susceptible to phagocytosis when compared to particles with sulphate, hydroxyl and/or carboxyl groups [41]. The surface hydrophobicity is a key factor for opsonization, affecting also phagocytosis, the circulation in blood, biodistribution, NPs' stability and interactions with cells [34]. Hydrophobic particles in the body are preferentially coated by plasma proteins, being more quickly cleared by MPS [28, 34]. Ideally, the NPs should have a hydrophilic surface to resist the adsorption of plasma proteins and avoid uptake by macrophages [30, 37]. This can be achieved by coating the surface of NPs with a hydrophilic polymer or directly fabricating NPs from block copolymers containing both hydrophilic and hydrophobic segments [30].

The surface of the NPs can be engineered to escape the MPS, improving their blood circulation half-life and biodistribution [35, 42]. PEGylation is a successful and commonly used approach for improving the efficiency of drug delivery to target cells and tissues, being the preferred method of

conveying stealth or sterically stabilized properties to NPs [28, 43]. PEGylation consists in the decoration of a particle surface by the covalently grafting, entrapping or adsorbing of poly(ethylene glycol) (PEG) chains [28, 44]. PEG presents several desirable characteristics, such as non-toxicity, non-immunogenicity and high water solubility [44]. Due to the hydrophilic nature of the ethylene glycol (EG) repeats they can extend into solution and shield the surface of the particle, being responsible for the PEGylated NPs' increased solubility [28, 45]. PEG groups onto the surface of particles enable stealth properties that can reduce nonspecific uptake by cells, reduce adsorption of biomolecules and avoid phagocytosis by macrophages, contributing to longer circulation time [26, 46]. The increase in circulation time is due to the very flexible and highly hydrophilic, neutral charge and flexible PEG chains [28]. PEG chains form a layer that has a repulsive effect preventing interactions with plasma proteins and the uptake from the MPS [28, 45]. The length and density of PEG chains strongly influence the NPs' protection against protein adsorption and, consequently, their stealth properties [47, 48]. It was demonstrated that long PEG chain length and high surface density provide better protein repulsion [49]. The PEG chains can acquire two different conformations, mushroom and brush (figure 2), depending on density [45, 47]. NPs with brush conformation have longer circulation time and are the most resistant to phagocytosis because the denser coatings better shield them from the MPS [45].

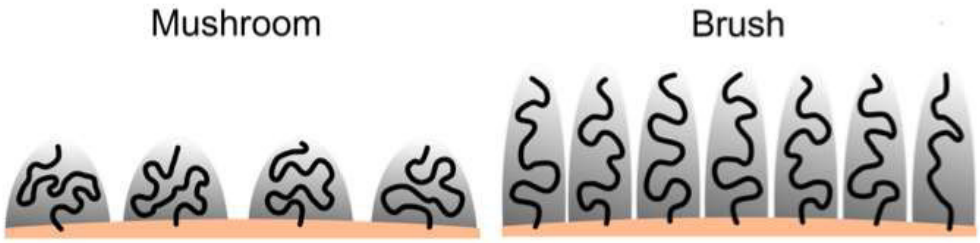

Figure 2 | Schematic representation of nanoparticle surface functionalized with PEG chains in mushroom and brush conformations [From Loureiro *et al.*, 2016 [2]].

1.2. Nanoparticles as drug delivery systems

NPs as DDS, are nanoscale particles, devices or systems decorated with special functionalities that can be made using a variety of materials, both organic and inorganic [50-52]. These therapeutic delivery systems have been developed based on several components, from metals to proteins, including carbon, silica oxides, metal oxides, nanocrystals, lipids, polymers, dendrimers and quantum dots [53, 54]. NPs include a vast number of structures such as lipid-based vehicles

including liposomes, solid lipid NPs and micelles; polymer carriers, such as hydrogels, polymersomes, dendrimers, polymeric NPs and nanofibers; metallic NPs; carbon structures such as nanotubes, nanohorns, nanodiamonds and graphene; and inorganic NPs such as silica (some of these structures can be seen in figure 3) [55, 56].

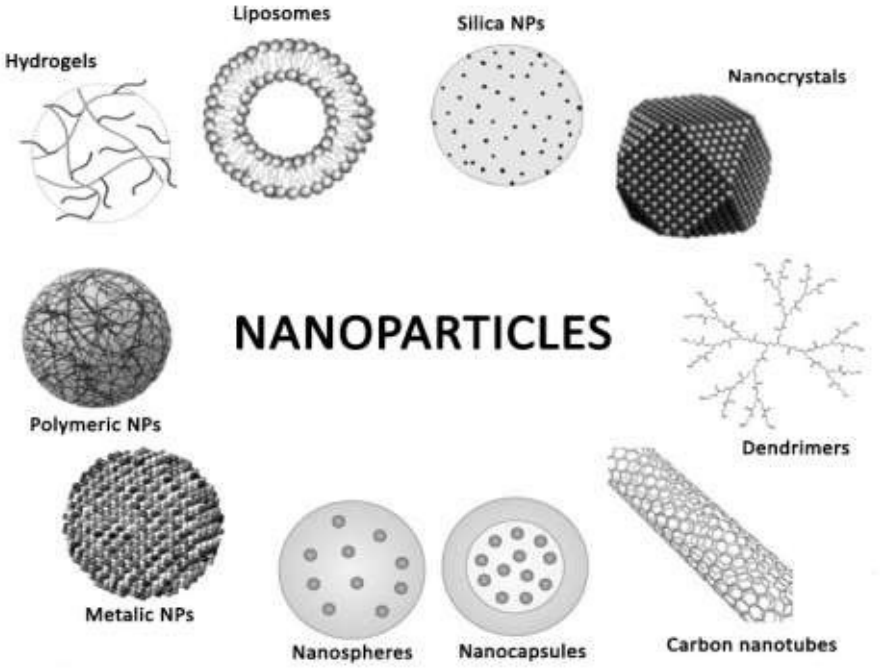

Figure 3 | Schematic view of different types of NPs [From Caban *et al.*, 2014 [56]].

In drug delivery, the most important NPs are liposomes, polymer conjugates, polymeric micelles, dendrimers, nanoshells, polymeric NPs and nucleic acid-based NPs [2]. However, liposomes and polymer-based nanoformulations constitute the majority (more than 80 %) of the nanoparticle based therapeutics available for clinical use [2, 54, 57].

1.2.1. Polymeric micelles

Polymeric NPs were first described in 1976, with the demonstration of a controlled release of macromolecules from biodegradable polymers [53]. In the production of these NPs, both natural (proteins and polysaccharides) and synthetic polymers can be used [58, 59]. Polymeric NPs are made from biocompatible and biodegradable materials and are designed to carry the drug with the objective of delivering this active molecule to the intended target [28, 55].

Polymeric micelles were first reported as drug delivery vehicles for cancer treatment in the early 80s [60-62], being recognized as one of the most potent and promising DDS in the 90s [62]. Since then, there has been the development of a great number of polymeric micelles for drug delivery [60, 61]. Polymeric micelles are colloidal particles based on block-copolymers with hydrophilic and hydrophobic units that self-assemble in an aqueous environment into nano-sized structures, usually within a range of 5–100 nm (figure 4) [63-66].

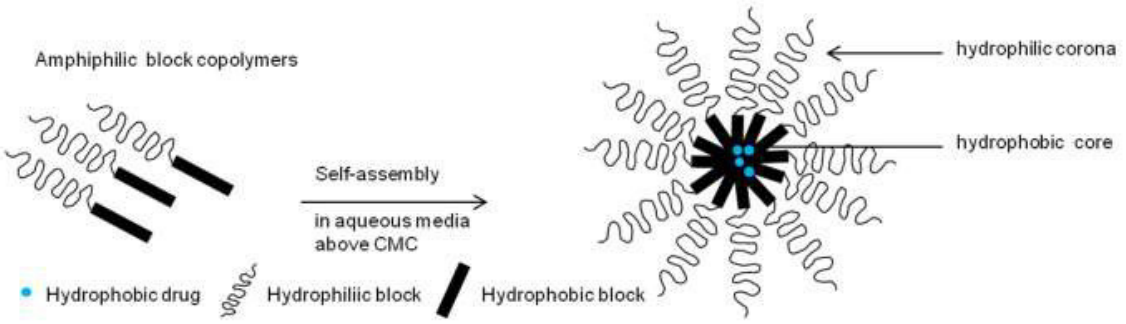

Figure 4 | Process of micelle formation and representation of micelles structure [From Jhaveri and Torchilin, 2014 [66]].

The hydrophilic shell of the micelles provides steric stability by creating a highly water-bound barrier, which blocks the adhesion of plasma proteins, avoiding the rapid uptake by MPS and resulting in a prolonged circulation time [63, 64, 67]. This outer hydrophilic shell is usually composed of PEG [68]. This compound is the premium choice because it is water soluble, biocompatible, uncharged and provides steric protection [69]. In micelles, PEG forms a dense, brush-like shell limiting the micelle interaction with other micelles and proteins, thus avoiding uptake and removal by the MPS [68]. The hydrophobic block serves as a nano-container responsible for the drug loading capacity of the micelles [63, 64, 67]. As the hydrophobic core is responsible for the encapsulation of poorly water-soluble drugs, it should be highly compatible with the incorporated drug and exhibit high loading capacity [68, 69]. In sum, the micelles outer shell is responsible for its pharmacokinetic profile, while its inner core determines drug stability, drug loading capacity and drug release behavior [70, 71].

In aqueous medium at low concentrations, the polymers exist as monomers but when the concentration increases, aggregation and self-assembly takes place resulting in the formation of micelles [63, 72]. The concentration at which micelles are formed is referred to as the critical micelle concentration (CMC) [63, 72]. In a concentration lower than the CMC, the polymers exist as monomers and at a concentration around or above the CMC, there is the micelles formation

[61]. The micelles formation above their CMC is driven by dehydration of the hydrophobic tails, leading to a favorable state of entropy [63]. Additionally, the formation of Van der Waals bonds allow the assembly of hydrophobic polymers to form the micelle core and the resulting hydrophilic shell re-establishes the hydrogen bonds with the surrounding water [63]. The CMC also provides information on the extent to which the micelles can withstand dilution [73]. This parameter depends mainly on the properties of the hydrophobic core [73, 74]. Increasing the hydrophobic part, i.e. the size of the hydrophobic block, results in a lower CMC value [73, 75] and the micelles stability is enhanced [74]. In sum, the lower is the CMC value of a polymer, the more stable are micelles [73, 76].

The formation of polymeric micelles involves two forces: an attractive force leading to the association of molecules and a repulsive force, which prevents the micelles unlimited growth [73]. After polymer synthesis, there are several techniques that can be used for the micelles formation and drug loading [77]. The formation of drug loaded polymeric micelles can occur by chemical conjugation or physical loading [62, 77, 78]. Chemical conjugation consists in the formation of a covalent bond between the drug and the micelles hydrophobic core, causing steric interference and resistance to enzymatic cleavage [62, 74]. Physical loading is based on hydrophobic interactions between the drug and micelles core [62]. Physical method is more advantageous for drug incorporation [74] and generally favored over chemical conjugation, especially in the case of hydrophobic drugs [79]. In the encapsulation of hydrophobic drugs the most used methods are the dialysis, oil-in-water emulsification, solvent evaporation and solid dispersion method [70, 77].

Drug release can occur by two major pathways, the micelles dissociation followed by the drug cleavage from the monomers and the drug cleavage within the micelle and its further diffusion out of the micelle [74, 80, 81]. In the case of a physically encapsulated drug, its release is usually proceeded by diffusion [80].

The ideal DDS should not present drug release during circulation, in fact, the drug should only be released after its accumulation at the target site and by some internal stimulus [60]. Therefore, the micelles core can be engineered in order to allow a controlled drug release [74]. This enables the development of stimuli-responsive nanocarriers which disassemble and release the drug to a specific biological environment in response to specific triggers [82, 83]. The triggers to which polymeric micelles can react include internal stimuli (pH, redox potential and a particular enzyme), as well as external stimuli (magnetic field, light, temperature and ultrasound) [60, 61, 82]. For example, the tumors present certain specific and unique features including low pH, overexpression

of specific enzymes, high levels of glutathione in the cytoplasm, as well as a higher temperature compared with the normal tissues [61, 83]. In this way, these characteristics present a great potential as internal triggers to destabilize stimuli-responsive micelles and achieve temporally and spatially controlled drug delivery and release in cancer therapy [61].

Polymeric micelles present great advantages as DDS because they can solubilize poorly soluble drugs and partly protect the drug from the aqueous environment [72], overcoming several problems of IV administration [63]. Moreover, their easy preparation, biocompatibility and their suitable characteristics that protect the drug from the biological environment, can improve the drug bioavailability and circulation time [84, 85]. These micelles also decrease the toxicity and other adverse effects associated to many drugs [76]. As polymeric micelles present all these promising and attractive features as efficient DDS, they have been receiving fast-increasing scientific attention [71]. Therefore, there are several formulations in clinical trials or already in the market, as it can be visualized in figure 5 [86].

Product	Incorporated drug	Status
Genexol PM	Paclitaxel	Marketed
Estrasorb	Estrogen	Marketed
Medicelle	DACH-platin-PEG-polyglutamic acid	phase I/II
Flucide	Anti-influenza	phase I/II
Basulin	Insulin	phase II/III
DO/NDR/02	Paclitaxel	phase I/II
NK-911	Doxorubicin	phase II
NK-105	Paclitaxel	phase II/III
NK-012	SN-38	phase II
NC-6004	Cisplatin	phase III
NC-4016	Oxaliplatin	phase I/II
SP-1049C	Doxorubicin	phase II/III
NC-6300	Epirubicin	phase I/II

Figure 5 | List of drug-loaded polymeric micelles-based products [Adapted from Kalepu and Nekkanti, 2015 [86]].

1.2.2. Liposomes

Liposomes were first discovered in the 1960s by Bangham, a British hematologist [87, 88]. Bangham was conducting experiments with phospholipids and blood clotting when he observed that phospholipids formed closed spherical bilayer structures spontaneously in aqueous medium [89-91]. It was also discovered later that those structures were hollow and could encapsulate drugs and thus be used as DDS [88, 91]. The structures were then designated as liposomes by Sessa and Weissmann, 1968 [89]. Its potential as DDS started in the 70s, becoming essential to research and clinical applications in the field of nanotechnology, especially nanomedicine [92, 93]. Liposomes are particularly ideal for drug delivery due to their similarity to natural cells [94]. Liposomes are defined as colloidal associations of amphiphilic lipids (phospholipids) that spontaneously organize themselves in bilayer vesicles in the presence of water, producing an aqueous medium surrounded by a lipid membrane (figure 6) [94-96]. They are spherical phospholipid vesicles which consist of one or more concentric lipid bilayers, with particle sizes ranging from 30 nm to several micrometers in diameter [97-99]. In the case of liposomes for medical purposes, its size ranges between 50 and 450 nm [100].

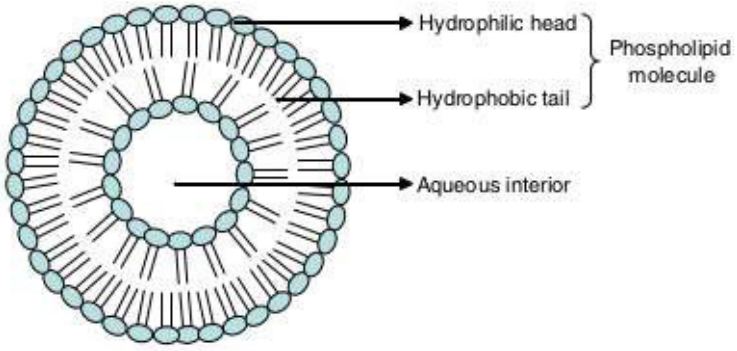

Figure 6 | Structure of a unilamellar liposome [From Swaminathan and Ehrhardt, 2011 [96]].

The formation of the lipid bilayer is due to the hydrophobic interactions, Van der Waals interactions that keep the hydrocarbon tails together and also the hydrogen bonds and polar interactions between the water molecules of the aqueous medium and the polar heads of lipids [88, 92, 100]. The final lipid bilayer organization depends on the nature, concentration, temperature and also the geometric form of the lipids [100]. Liposome properties and its therapeutic action can vary according to lipid composition, size, surface charge and preparation method [101]. Several methods have been reported for liposome preparation and each one of them influences its

properties such as size, number of bilayers, encapsulation efficiency (EE) [92], shape and stability [89]. These methods are divided into three categories: mechanical methods (preparation by film methods and homogenization techniques), methods based on the use of organic solvents (ethanol injection method and reverse-phase evaporation) and methods based on detergent depletion (dialysis) [102].

Currently, liposomes are one of the most common and frequently used nanoparticle encapsulation systems for targeted drug delivery [98, 100, 103]. Its potential is also due to the fact that liposomes can encapsulate and effectively incorporate both hydrophilic and hydrophobic substances [95, 102, 104]. Hydrophilic compounds can be incorporated in the inner aqueous core while hydrophobic compounds can be carried inside of the lipid bilayer (hydrophobic domain) [42]. These type of DDS presents mainly numerous advantages, however there are still some drawbacks associated, as shown in table 1.

Table 1 | Advantages and disadvantages of liposomes

Advantages of liposomes [87, 92-94, 101, 105]	Disadvantages of liposomes [87, 101]
• Increased efficacy and therapeutic action of drug • Improved drug stability • Non-toxic, flexible, biocompatible, biodegradable and non-immunogenic • Simplicity of production • Decreased drug toxicity • Controlled release properties • Reduction of the nonspecific side-effects • Specific targeting to specific cells or tissues	• High production cost • Leakage and fusion of encapsulated drug/molecules • Short half-life • Low solubility • Sometimes phospholipid undergoes oxidation and hydrolysis-like reactions

Liposomes can be designed in order to overcome several associated drawbacks and to obtain desirable and adequate characteristics, improving their therapeutic effect [91]. For example, the addition of cholesterol to the lipid bilayer allows to enhance the stability of liposomes, reduce the permeability to water soluble molecules and increase the fluidity or microviscosity of the bilayer [90, 104, 106]. Cholesterol also prevents the interaction and destabilization of liposomes by blood proteins [88, 94, 106]. In general, its role is to stabilize the lipid bilayer [92, 106]. The stability and circulatory time in the bloodstream of liposomal formulations can also be improved by biocompatible and hydrophilic polymers with a flexible main chain, such as PEG [94]. A widely used approach is the coating of the liposome surface with a lipid derivative of PEG [87, 107], being

the 1,2-distearoyl-sn-glycero-3-phosphoethanolamine (DSPE) a phospholipid widely used in conjugation with PEG [89].

There are several liposomal-based therapies approved by Food and Drug Administration (FDA) which are intended for several therapeutic purposes, such as cancer therapy, treatments against fungi or microbes, for vaccination, analgesia, macular degeneration and hormone replacement [88], represented in figure 7. The first liposomal anticancer drug approved was Doxil®, introduced in the USA market in 1995 [105, 108]. Subsequently, it were introduced more products for cancer treatment such as DaunoXome®, Depocyt®, Myocet®, Mepact®, Marqibo® and Onivyde™ [108, 109]. Also, it were developed other products for other medical purposes such as fungal infections (Abelcet®, Ambisome® and Amphotec®), photodynamic therapy (Visudyne®), pain management (DepoDur™ and Exparel®) and viral infections (Epaxal® and Inflexal® V) [108].

Figure 7 | Marketed liposomal formulations and respective areas of application [From Bulbake *et al.*, 2017 [108]].

2. NANOPARTICLES AS AN EMERGING PLATFORM FOR CANCER THERAPY

Cancer is a term used for a large group of diseases, in which abnormal cells divide in an uncontrolled manner beyond their usual boundaries and are able to invade and spread to other tissues or organs [63, 110]. These changes are the result of the interaction between a person's

genetic factors and three categories of external agents, including physical carcinogens, chemical carcinogens and biological carcinogens [111]. Cancer has become one of the most devastating and life-threatening diseases, causing a large number of deaths worldwide [110, 111]. The most predominant and common cancer treatments include chemotherapy, radiation and surgery [110, 112]. However, the conventional chemotherapeutic agents still exhibit poor specificity in reaching tumor tissue, causing significant damage to normal tissues and resulting in undesirable side effects [113, 114]. There is the need to develop new modalities for cancer treatment that can either passively or actively target cancer cells, enhancing the intracellular concentrations of drugs in cancer cells while avoiding toxicity in normal cells [2, 51, 115]. The combination of controlled release and targeted drug delivery has allowed the emerging of NPs as an efficient and inoffensive solution to overcome the limitations found in conventional cancer therapy [113, 116]. It's demonstrated in the literature that NPs have made a tremendous impact in the treatment of various types of cancer, as evidenced by the numerous nanoparticle-based drugs and delivery systems that are in clinical use [117]. NPs possess several advantages as DDS in cancer (figure 8): they can evade the immune system and selectively deliver high concentrations of drugs to tumor cells, greatly reducing or eliminating the side effects and increasing the efficacy of the treatment [118]. NPs can also maintain the drug levels within a desired range, needing fewer administrations and providing an optimal use of the drug and increase patient compliance [113]. Additionally, NPs can overcome multidrug resistance (MDR) and can improve aqueous solubility of anticancer drugs, which results in increased bioavailability [112]. NPs may also be engineered to have a prolonged circulation time and to have enhanced cellular uptake and targeting abilities [22]. The attachment of targeting ligands to the surface is one of the most used strategies to improve circulation time of NPs and to enhance their uptake by target tissues [42]. In conclusion, NPs are a successful method for the delivery of anticancer agents to cancer cells or tissues [118].

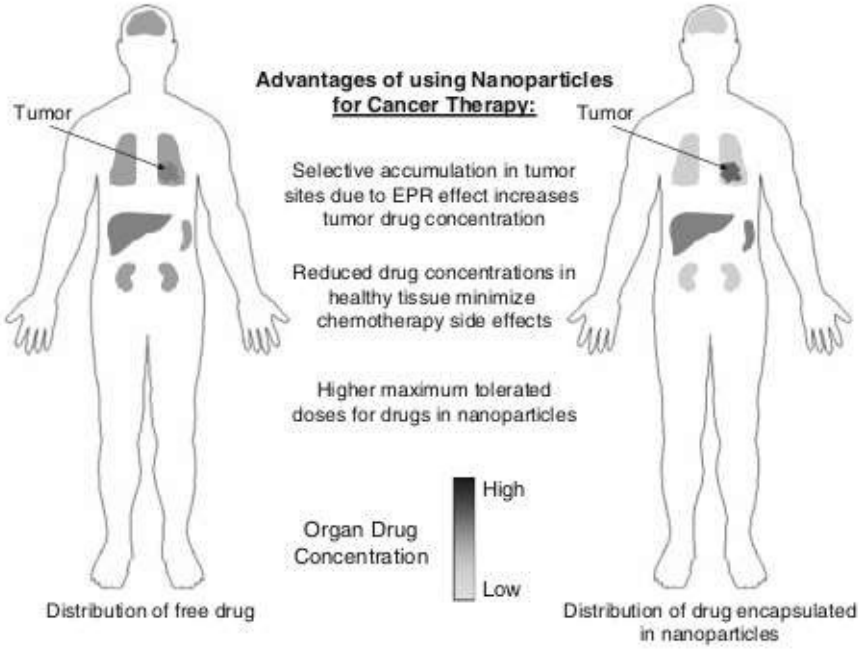

Figure 8 | Advantages of using NPs as DDS for cancer therapy compared to free drug [From Alexis *et al.*, 2010 [42]].

Passive delivery consists in the NPs' transport through leaky tumor capillary fenestrations into the tumor interstitium and cells by passive diffusion (transport of molecules through the membrane, per the concentration gradient) or convection (movement of molecules within fluids) (figure 9) [35, 119]. The tumor demonstrates a high vascular density, which is irregularly branched and disorganized, increasing vascular permeability and inefficient lymphatic drainage [119-121]. These characteristics allow the accumulation of the NPs and the drug in tumor tissue by enhanced permeation and retention (EPR) effect [35, 122]. The passive targeting process is influenced by factors such as particle composition, size, shape and surface characteristics [120]. NPs can be designed regarding these physicochemical characteristics to better target a particular tissue or cell [120].

In several pathological situations, the integrity of vascular endothelium remains unaffected, which results in the absence of the EPR effect [115, 123]. Moreover, the permeability of vessels may vary throughout the tumor [115]. So, in order to overcome these limitations, it is used the strategy of active targeting [115]. Active targeting involves drug delivery to a specific site based on molecular recognition [35, 120]. This strategy encompasses the coupling of a ligand to a nanoparticle via covalent and non-covalent methods, enabling the interaction of the ligand with its receptor at the target (figure 9) [35, 120]. The ligand incorporation facilitates the entry of NPs to cancer cells via receptor-mediated endocytosis, allowing the release of the drug and providing a therapeutic action

[124]. In active targeting, it can be used several ligands such as proteins (antibodies and their molecular fragments), nucleic acids (aptamers) and small molecules (vitamins, peptides or carbohydrates) [120, 124]. The choice of target receptor on the cancer cells is an important factor of this strategy [125]. The target receptors should present some desirable characteristics, such as be expressed more selectively as possible or uniquely on tumor cells and must be present in a high quantity on the cell's surface [116, 119, 125].

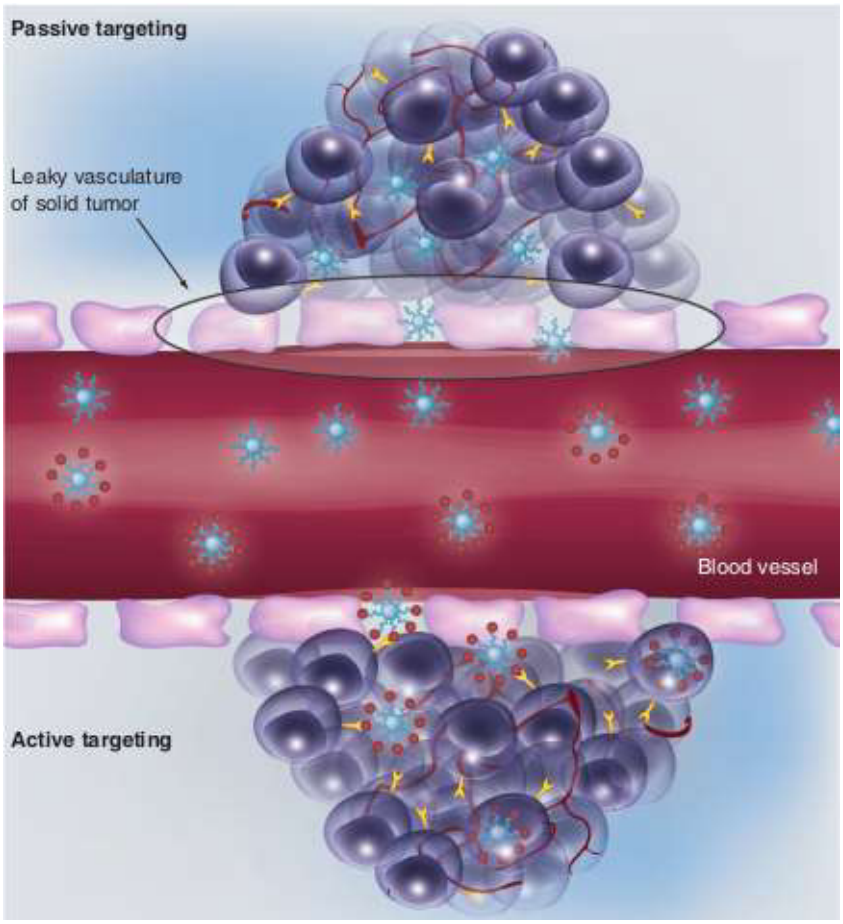

Figure 9 | Passive and active targeting for drug delivery to solid tumors [From Huynh *et al.*, 2010 [121]].

The monoclonal antibodies are the most frequently used targeting agents in active targeting because they can be used against characteristic components of target organs or tissues [123]. Currently, human monoclonal antibodies can be used against virtually any target protein of interest, and certain antibodies have exhibited a remarkable ability to selectively confine in solid tumors [126]. More than 30 antibody-drug conjugates are in clinical testing, mostly for applications in cancer [126]. Nevertheless, these antibodies present limitations, such as their immunogenicity and they do not extravasate and diffuse efficiently into tumor tissue, leading to the exploration of

alternative strategies for the targeted delivery of drugs [126]. The use of peptides, sugars and small molecules, such as vitamins, is a more attractive approach than antibodies [42, 126]. These small molecules demonstrate desirable characteristics, such as high stability, high purity, ease of production and non-immunogenicity [42, 126]. The use of vitamins, such as FA, vitamin B12, biotin and thiamine, as a target ligand for drug delivery has been quite prominent [110]. FA targeting is an interesting approach for cancer therapy because it offers several advantages over the use of monoclonal antibodies, including their non-immunogenicity and rapid internalization via receptor-mediated endocytosis [110, 127]. FA also presents the advantages of being stable in storage and circulation, inexpensive, non-toxic, it can be conjugated easily to the carrier and has a very high affinity for folate receptor (FR) [110]. FA is a water soluble vitamin required in one carbon metabolism pathways, for example in the synthesis of purines and pyrimidines in order to generate deoxyribonucleic acid (DNA) and ribonucleic acid (RNA) and in the synthesis of several amino acids [110, 128-130]. Therefore, FA is a nutrient essential for cellular division, especially in many tumors due to their rapid cell division cycles, requiring a greater amount of vitamins needed for biosynthesis and nutrient metabolism [126]. FA enters normal cells through the reduced folate carrier, an anion transporter that delivers FA across the plasma membrane in a bidirectional manner, but FA conjugates only enter in the cells through the FR via receptor-mediated endocytosis [129, 130]. Human FR has three well characterized isoforms: FR-α, -β, and -γ [130]. FR-α is overexpressed on many types of cancer cells while FR-β is overexpressed on activated macrophages, implicated in inflammatory pathologies, and also on the surface of malignant cells of hematopoietic origin [130, 131]. FR-γ is overexpressed in various types of human cancers, especially on many epithelial cancers [128, 131]. The expression of the several isoforms of FRs is highly restricted among human tissues, in particular the expression of FR-α [128]. The healthy tissues that express FR-α include the proximal tubules of the kidney and apical surfaces of several epithelial cells [131]. These apical surfaces of epithelial cells are inaccessible to intravenously administered FA and FA conjugates [130, 131]. However in the kidney, FR-α expressed in the proximal tubules will bind to targeted agents that are filtered from the blood stream [130, 131]. As FR is practically absent in most normal tissues and is frequently overexpressed in various types of human cancers, this receptor is a possible target for a number of types of cancer [132]. It has been described that FA and its derivatives bind with high affinity to FR-α, that mediates their internalization by endocytosis [128], being a great and promising targeting strategy for cancer therapy [110]. Therefore, FA conjugates, including FA-tagged NPs, can deliver a variety of drugs to

pathological cells without causing harm to normal tissues, overcoming the side effects greatly associated with conventional cancer therapy [110, 127].

3. METHOTREXATE AS AN ANTICANCER DRUG

MTX, synthetized in the 1940s [133, 134], is one of the most effective drugs in the treatment of a wide range of health problems [135]. Since the 50s, the MTX has been clinically used in the treatment of many tumors and diseases [136] such as acute lymphoblastic leukemia, osteosarcoma, breast, head, lung, bladder and neck cancers, lymphoma, choriocarcinoma, trophoblastic neoplasms and psoriasis [137-139]. Although MTX is one of the most widely used drugs in cancer therapy [136, 140], this compound is also effective for the treatment of rheumatoid arthritis and other autoimmune diseases [133].

In general, MTX acts by inhibiting dihydrofolate reductase, an enzyme essential in the biosynthesis of thymidylate (TMP) [135, 140], which result in an inhibition of nucleic acid synthesis inducing cell death [137]. As it can be seen in figure 10, MTX enters the cell through the reduced folate carrier (a) and/or using an endocytic pathway activated by a FR (b) [141]. Afterwards it is polyglutamated by the folylpolyglutamate synthase enzyme (c) [134, 141]. Inhibition of the enzyme dihydrofolate reductase (d) is done by MTX and its polyglutamates, which prevents the conversion of dihydrofolate (FH_2) to tetrahydrofolate (FH_4) [134, 141]. In this way, it results in a reduction of TMP synthesis (e), inhibiting DNA synthesis (f) [134, 141]. Long-chain polyglutamates of MTX have increased inhibitory effects on both TMP synthesis (e) and purine biosynthesis (f), which is required for RNA production [141].

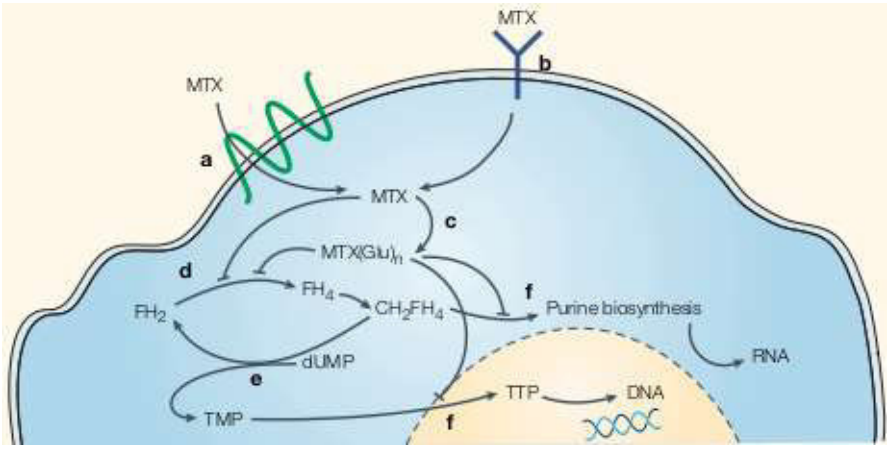

Figure 10 | Mechanism of action of MTX. MTX enters the cell through the reduced folate carrier (a) and/or using an endocytic pathway activated by a FR (b). Afterwards it is polyglutamated by the folylpolyglutamate synthase enzyme (c). Inhibition of the enzyme dihydrofolate reductase (d) is done by MTX and its polyglutamates, which prevents the conversion of FH_2 to FH_4. This causes a reduction of TMP synthesis (e), thus inhibiting DNA and/or RNA synthesis (f) [From Chabner and Roberts Jr, 2005 [141]].

MTX therapy presents some limitations, such as high toxicity toward normal cells due to its low specificity and short plasma half-life [136, 140], drug resistance, poor water solubility [138], nephrotoxicity, bone marrow suppression, hepatotoxicity and leukopenia [135, 139]. In this way, it is often required the dose reduction or even the withdrawal of the treatment [137]. Therefore, it is necessary the development of approaches that can overcome the limitations of the MTX and improve its therapeutic efficacy [138]. One solution developed was the conjugation of MTX with monoclonal antibodies, which enables the selectivity of MTX to the tumor site [140]. However, this strategy also presented limitations such as immune response against the antibodies and also the fact that antigens are present in normal tissue and in the blood stream [140]. Another strategy was the coupling of the drug to macromolecules, increasing its MW and resulting in an accumulation at the tumor site [140]. Nevertheless, the most promising approach is the use of DDS for MTX delivery to the tumor site [139, 140], such as liposomes and polymeric micelles [135].

In the present work, it was developed two types of NPs (polymeric micelles and liposomes) with suitable characteristics for application as DDS in cancer therapy. In order to encapsulate the MTX in the hydrophobic core of the micelles and in the lipid bilayer of the liposomes, were produced hydrophobic MTX derivatives. Moreover, in the literature, it is found that an overall reduction in the polarity of MTX is important to enhance passive internalization of this cytotoxic agent [142]. The modification of one or both carboxyl groups, present in the glutamate moiety of the MTX molecule, appeared to be a good approach because it does not interfere with the binding of MTX to its target [142].

CHAPTER III

Development of PEGylated micelles for hydrophobic methotrexate delivery

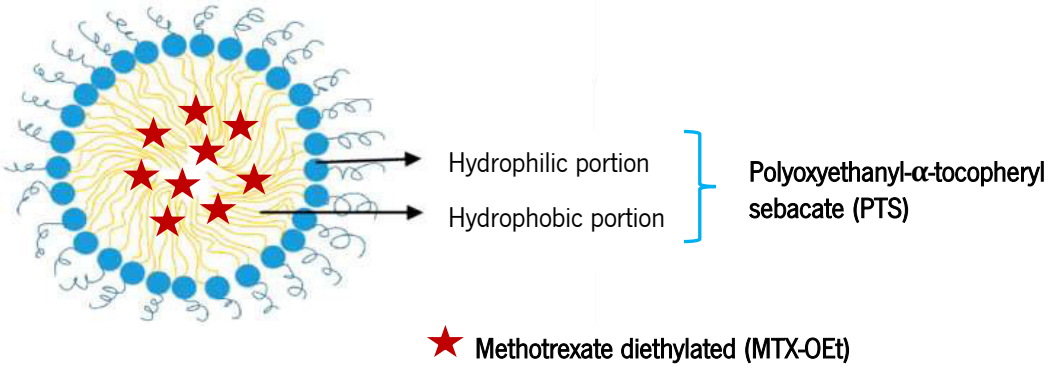

Chapter III – DEVELOPMENT OF PEGYLATED MICELLES FOR HYDROPHOBIC METHOTREXATE DELIVERY

1. FRAMEWORK

In this chapter, is described the development of PEGylated micelles produced using polyoxyethanyl-α-tocopheryl sebacate (PTS), a PEG derivative. This compound facilitates the formation of nanomicelles due to its self-emulsifying properties [143]. PTS is an amphiphilic compound that possesses both hydrophilic (PEG) and hydrophobic/lipophilic (α-tocopherol) properties, separated by an aliphatic spacer (sebacic acid) (figure 11) [143, 144].

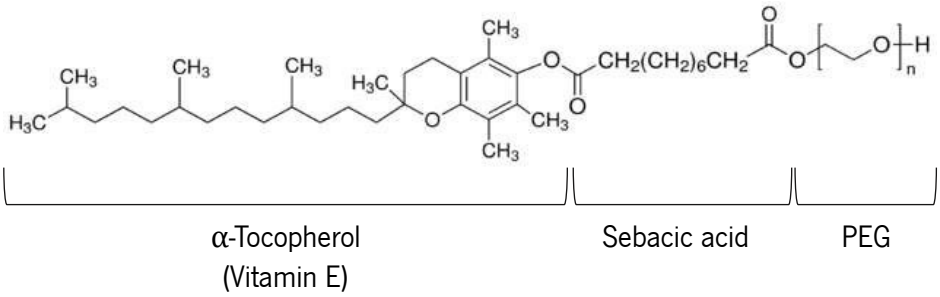

Figure 11 | Structure of PTS and its respective components: α-tocopherol, sebacic acid and PEG.

PTS also presents several advantages as a solubilizing agent for numerous lipophilic bioactive molecules, such as lack of toxicity, maximum solubilizing ability and stealth properties [144, 145], being appropriate for rapid delivery, namely intravenously [145].

To produce the PTS compound, the highly hydrophobic and lipophilic molecule of α-tocopherol is esterified with hydrophilic molecules, such as sebacic acid and PEG [145]. PTS, as an esterified form of α-tocopherol or vitamin E, is able to release an active form of this vitamin when systemically metabolized [144]. Vitamin E is an essential micronutrient in the preservation of the balance between antioxidant and pro-oxidant reactions in tissues [67, 146]. This vitamin has numerous functions including antioxidant, anti-inflammatory, anti-thrombotic, hypocholesterolemic and anti-carcinogenic [72, 143, 144]. It was also discovered recently that vitamin E has potent anti-tumorigenic activity by inducing apoptosis in several cancer cell lines [146]. The use of vitamin E derivatives-based nanomedicines in the treatment of cancer demonstrates potential as a novel anticancer treatment [72]. Moreover, these nanomedicines are currently under investigation as carriers for hydrophobic drugs to improve anticancer therapy efficacy [63]. In this work, besides

the development of PEGylated micelles using PTS it was also optimized the entrapment of a hydrophobic derivative of MTX, MTX-OEt.

Water-soluble micelles were prepared using PTS in the presence (auxiliary solvent method) or absence (sonication method) of an organic solvent. An optimization of these two methods for micelles preparation was performed, testing different conditions in order to prepare PEGylated micelles with suitable characteristics for drug delivery. Subsequently, the full characterization of the developed micelles and the evaluation of the biological effect of these micelles loaded with MTX-OEt were performed.

In this way, with this work it is hoped the development of promising PEGylated micelles that can improve the drug's efficacy and safety, overcoming the physiological barriers and the several limitations associated with conventional therapies.

2. MATERIALS AND METHODS

2.1. Reagents and Equipment

2.1.1. Reagents

The main components used for micelles preparation were PTS and MTX. MTX was purchased from TCI Chemicals (Belgium). PTS was produced in the laboratory and for that the following reagents were needed: ethyl acetate and methanol from Fisher Chemical (UK); DL-(+)-α-tocopherol, triethylamine (TEA) and PEG 600 from TCI Chemicals (Belgium); sebacoyl chloride from Honeywell Fluka™ (USA); and a 26.67 % saturated NaCl (Labbox, Spain) solution. Commercial PTS was obtained at 15 wt. % in water from Sigma-Aldrich (USA). Throughout the preparation process several solvents were used, such as: acetone acquired from Fisher Chemical (UK); phosphate buffered saline (PBS) purchased from Biochrom GmbH (Germany) and ultrapure water was obtained from a Milli-Q Water Purification System (Germany).

Tangential filtration needed specific solutions such as a 0.05 M NaOH solution for the systems' maintenance and 0.5 M NaOH solution for systems' rinsing, both from Sigma-Aldrich (USA). Dialysis tubes with a molecular weight cut-off (MWCO) of 1 kDa were purchased from Sigma-Aldrich (USA).

For the characterization of the developed micelles through proton nuclear magnetic resonance (^{1}H NMR) spectroscopy was used deuterated dimethylsulfoxide (DMSO-d_6) as a deuterated solvent, which was purchased from Cortecnet (France). Pyridine was used as internal standard for drug quantification and was purchased from Sigma-Aldrich (USA). For the characterization through matrix-assisted laser desorption/ionization time-of-flight (MALDI-TOF) was used 2,5-dihydroxybenzoic acid (DHB) and super-DHB as matrix, trifluoroacetic acid and NaOH that were purchased from Sigma-Aldrich (USA). Acetonitrile (high-performance liquid chromatography (HPLC) grade) and HCl 37 % were obtained from Fisher Scientific (USA).

To perform cellular tests, the micelles were filtered under sterile conditions using 0.22 μm polyethersulfone (PES) filter, purchased from Merck Millipore (Ireland). Human skin fibroblasts (BJ5ta cell line) and human colorectal adenocarcinoma cells (Caco-2 cell line), obtained from American Type Culture Collection (ATCC) (UK), were the chosen cell lines to test the biological effect of micelles. T75 cell culture flasks and 96-well tissue culture polystyrene plates were purchased from SPL Life Sciences (Korea). All culture media and supplements were purchased

from Sigma-Aldrich (USA). The cell viability tests were performed using Promega CellTiter 96® AQueous Non-Radioactive Cell Proliferation 3-(4,5-dimethylthiazol-2-yl)-5-(3-carboxymethoxyphenyl)-2-(4-sulfophenyl)-2*H*-tetrazolium (MTS) assay, which was purchased from Promega (USA).

2.1.2. Equipment

Two different methods were used in the micelles production. The auxiliary solvent method involves the addition of an organic solvent (acetone). In this way it was necessary a step of evaporation which was performed using a Hei-VAP G3 rotary evaporator from Heidolph (Germany). In order to eliminate the presence of the organic solvent in the micelles production process, the sonication was used as an alternative method. The sonication was performed using a VC 505/VC 750 Sonics Vibracell Ultrasonic Processor and the probe was the 20 kHz Vibracell CV 33, 3 mm diameter titanium from Sonics & Materials (USA).

PD-10 sephadex desalting columns with a MWCO of 5 kDa were used for the separation of free drug from the micelles. Another separation method performed was the tangential flow filtration (10 kDa MWCO, 20 cm^2, modified polyethersulfone (mPES) module, with a 27 mL/min feed) using a KrosFlo® Research 2i Tangential Flow Filtration (KR2i TFF) System from Repligen (USA). Ultrafiltration was another separation method tested, which was performed using a solvent-resistant stirred cell with Ultracel 10 kDa regenerated cellulose ultrafiltration discs, 47 mm (Merck Millipore, Ireland).

Full characterization of the developed micelles was performed by analyzing several parameters through the use of different equipment. Dynamic light scattering (DLS) analysis was performed using a Malvern Zetasizer Nano ZS from Malvern Panalytical (UK). All spectroscopic measurements were conducted in a Synergy Mx Multi-Mode Reader from BioTek (USA). The samples used for NMR analysis were lyophilized using a Lyophilizer FreeZone 2.5, purchased from Labconco® (USA). ^{1}H NMR spectra were recorded using a Bruker Avance III 400 (Bruker Daltonics GmbH). MALDI-TOF mass spectra were acquired on a Bruker Autoflex Speed instrument (Bruker Daltonics GmbH). Fourier-transform infrared (FTIR) spectroscopy of PTS was obtained with a FT-IR Bomem MB from ABB (Switzerland). All cellular tests were performed using a ScanLaf Mars laminar flow chamber from Labogene (Denmark) and the cell cultures were maintained in Thermo Heraeus HeraCell 150 CO_2 Incubator from Hofstra Group (USA).

2.2. Production and characterization of the hydrophobic drug, MTX-OEt

This modified MTX was produced by a colleague in the laboratory (unpublished work). This compound was characterized by ^{1}H NMR and MALDI-TOF. In the ^{1}H NMR spectroscopy of MTX-OEt was used DMSO-d_6 as deuterated solvent. MALDI-TOF mass spectrum of MTX-OEt was performed using DHB as the matrix. A saturated solution of DHB was mixed with a 0.1 % solution of trifluoroacetic acid/acetonitrile (70:30) containing the sample. The samples were analyzed using the linear positive mode.

The absorbance spectrum of MTX-OEt was achieved in order to verify if the wavelength of maximum absorbance is the same of non-modified MTX (λ= 303 nm).

2.3. Preparation and characterization of PTS

2.3.1. Synthesis of PTS

The synthesis of PTS was performed according to Borowy-Borowski *et al.*, 2004 [144]. Initially, a solution of α-tocopherol in dry ethyl acetate was mixed with TEA. Afterwards, this solution was added to sebacoyl chloride dissolved in dry ethyl acetate, in an ice bath. After addition of the solution, the reaction proceeded at room temperature (RT) for 5 min. Then, a solution of PEG 600 in dry ethyl acetate with TEA was added to the previous mixture and the reaction was stopped with water after 10 minutes at RT with constant stirring. The reaction mixture was then washed with a saturated NaCl solution and the organic layer was concentrated in a rotary evaporator. The final solution was incubated overnight at 4 °C in order to precipitate the salts, which were removed by filtration. The filtrate was also concentrated under reduced pressure and dissolved in methanol, and incubated overnight at 4 °C to precipitate dimeric impurities. Finally, the supernatant was filtrated and the solvent was removed by evaporation. The final reaction product was dissolved in water, lyophilized, and the obtained yellow oil characterized through ^{1}H NMR spectroscopy and MALDI-TOF. The yield of the reaction was approximately η= 60.7 %.

2.3.2. Characterization of PTS

2.3.2.1. ^{1}H NMR spectroscopy analysis

^{1}H NMR spectroscopy of PTS was performed using DMSO-d_6 as a deuterated solvent and the peak solvent was used as internal reference.

2.3.2.2. MALDI-TOF analysis

MALDI-TOF mass spectrum of PTS was performed using super-DHB as matrix. A saturated solution of super-DHB was mixed with a 0.1 % solution of trifluoroacetic acid/acetonitrile (70:30) containing the sample. The samples were then analyzed using the linear negative mode.

2.3.2.3. FTIR analysis

FTIR spectrum of the PTS was verified using NaCl cells and previously lyophilized PTS. The spectrum was obtained in the region of ν= 400–4500 cm^{-1} at RT.

2.3.2.4. Absorbance measurements

The absorbance of PTS was measured from a wavelength of 250 to 750 nm in order to obtain the absorbance spectrum. Through the analysis of the obtained spectrum it was possible to determine if PTS could interfere in the drug quantification by absorbance.

2.4. Production of PTS micelles loaded with MTX-OEt

For micelles production were tested two different methods in order to prepare PEGylated micelles with suitable characteristics for drug delivery.

2.4.1. Auxiliary solvent method

PTS was dissolved in a mixture of acetone/ultrapure water and homogenized using vortex. The solution was subjected to evaporation at several temperatures (30, 40 and 50 °C) and at 100 rpm, using the rotary evaporator. For the production of PTS micelles loaded with MTX, the hydrophobic derivative MTX-OEt and PTS were dissolved in the initial mixture of acetone/ultrapure water.

Several ratios (w/w) of PTS/MTX-OEt were tested in order to produce the most promising micelles. After the evaporation of the acetone, the produced micelles were separated of the free drug using several separation methods (separation using dialysis tubes, desalting columns, amicons, ultrafiltration system and also the tangential filtration). The tangential flow filtration (10 kDa MWCO, 20 cm^2, mPES module, 27 mL/min feed) demonstrated to be the best method. This method allowed an efficient removal of free drug and PTS that were not incorporated in micelles, using water/PBS as eluent. Finally, the micelles were filtered under sterile conditions using 0.22 μm PES filter.

2.4.2. Sonication method

PTS was dissolved in ultrapure water and the solution was subjected to ultrasounds for 3 minutes using a high-intensity ultrasonic horn with an amplitude of 40 %, with and without controlled temperature (60 °C). For the preparation of micelles loaded with MTX was added MTX-OEt to the initial mixture, testing several ratios PTS/MTX-OEt (w/w). After micelles production, a separation of phases was performed by tangential flow filtration (10 kDa MWCO, 20 cm^2, mPES module, 27 mL/min feed), previously described as the best separation method for this type of NPs. The micelles were filtered under sterile conditions using 0.22 μm PES filter.

2.5. Characterization of PTS micelles loaded with MTX-OEt

2.5.1. Physicochemical characterization

The PTS micelles were analyzed by DLS. Using the Malvern Zetasizer, the size distribution and zeta-potential were analyzed at pH 7.4 and at 25 °C by photon correlation spectroscopy (PCS) and electrophoretic laser Doppler anemometry, respectively. The values for viscosity and refractive index were taken as 0.8616 cP (PBS)/0.8872 cP (water) and 1.333, respectively. PTS concentration was kept constant at 1 mg/mL. Micelle formulations were stored at 4 °C for a period of 8 weeks and their physicochemical parameters were periodically measured in order to study the NPs stability.

2.5.2. Determination of the encapsulation efficiency

The encapsulated drug was quantified by measuring the absorbance of the micelles solution after separation of the free drug at λ= 303 nm. A calibration curve was made and using the equation of this curve, the concentration of the drug was calculated. The EE was calculated using the equation 1, where $[drug]_{encapsulated}$ is the total concentration of drug present in the formulation after the separation process and the $[drug]_{initial}$ is the total concentration of drug added to the initial formulation.

$$Encapsulation\ efficiency\ (\%) = \frac{[drug]_{encapsulated}}{[drug]_{initial}} * 100$$

Equation 1 | Determination of EE.

2.5.3. Biological Characterization of the developed micelles

2.5.3.1. Cell cultures and conditions

In this work, the cellular tests were performed using BJ5ta and Caco-2 adherent cell lines, grown in T75 flasks and maintained under a humidified atmosphere of 5 % CO_2 in air and at 37 °C. Each cell line required specific media conditions, which are detailed in table 2.

Table 2 | Composition of cell culture media and supplements used for BJ5ta and Caco-2 cell lines

Cell Line	Media	Supplements
BJ5ta	4 parts of Dulbecco's Modified Eagle's Medium (DMEM) 1 part of M199 Medium	10 % (v/v) of Fetal bovine serum (FBS); 1 % (v/v) of penicillin/streptomycin solution; 10 µg/mL of hygromycin B
Caco-2	DMEM	20 % (v/v) of FBS; 1 % (v/v) of penicillin/streptomycin solution; 1 % (v/v) of non-essential aminoacids

Adherent BJ5ta and Caco-2 cell lines should present a fibroblast-like and epithelial-like morphologies [147, 148], respectively, which are represented in figure 12. These morphologies indicated that the cell lines were in good conditions and suitable to proceed with the biological

assays. BJ5ta cell line was used to test the cytotoxicity of the empty PTS micelles in normal cells. On the other hand, the Caco-2 cell line was used to test the biological effect of the developed micelles loaded with the pharmacological compound (MTX-OEt).

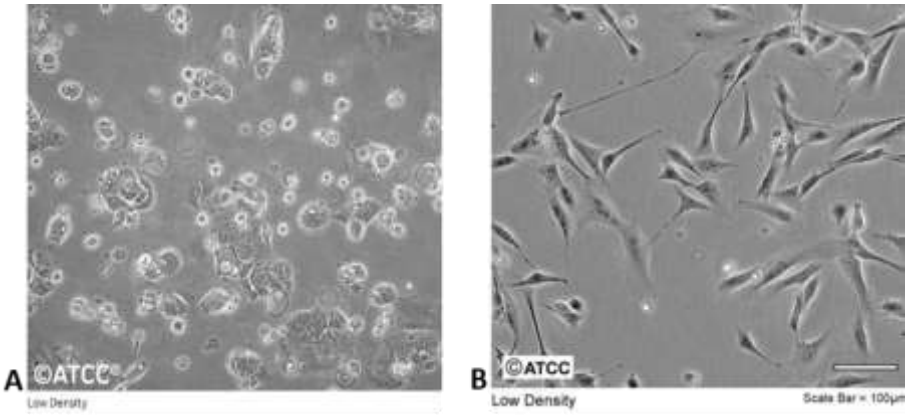

Figure 12 | Morphology of A) Caco-2 cell line and B) BJ5ta cell line [From ATCC, 2016 [147, 148]].

2.5.3.2.Cell Viability Assay

Cell viability was tested using the Cell Proliferation MTS assay, a colorimetric method for the assessment of cell viability [149, 150]. In this assay the viable cells convert MTS tetrazolium to formazan, a colored dye that is soluble in tissue culture medium (figure 13) [149, 150]. The formazan is then quantified by measuring the absorbance at 490 nm, enabling the calculation of the cell viability [149].

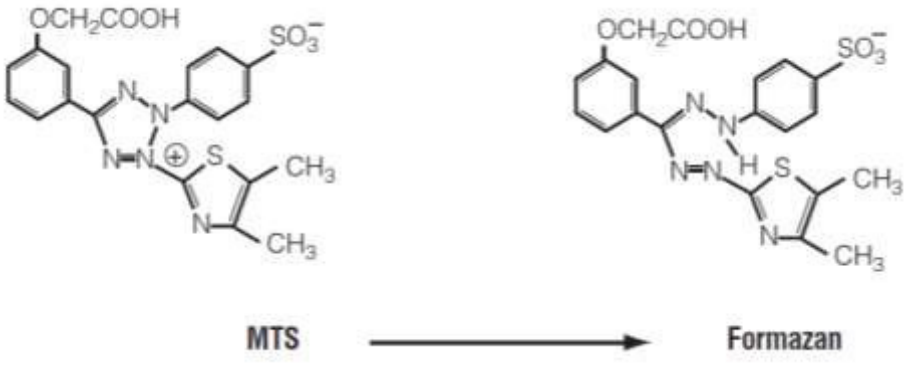

Figure 13 | Conversion of MTS into aqueous and soluble formazan, which is accomplished by dehydrogenase enzymes found in metabolically active cells [From Promega Corporation, 2018 [149]].

BJ5ta and Caco-2 cells were seeded in 96-well tissue culture polystyrene plates at a density of 1×10^4 cells/well and incubated overnight to promote cell adhesion. In the case of the cytotoxicity evaluation in normal cells (BJ5ta), the micelles without the drug were applied at different PTS concentrations (from 0.05 up to 1.50 mg/mL) for 72 hours at 37 °C. For the determination of biological effect, the Caco-2 cells were incubated with different concentrations (3 and 6 μg/mL) of free MTX-OEt and micelles loaded with the same concentrations of the drug, as well as with empty micelles as control, for 72 hours at 37 °C. After the incubation of the cells with all the different conditions, a MTS mixture was added to each well. The cells were further incubated for 4 hours at 37 °C, and finally, the absorbance of the formazan product was read at 490 nm. Cell viability was calculated using equation 2 and expressed as a percentage relative to the negative control, the untreated cells.

$$Cell\ viability\ (\%) = \frac{Absorbance\ of\ sample\ (mean)}{Absorbance\ of\ control\ (mean)} * 100$$

Equation 2 | Determination of cell viability as a percentage relative to the negative control.

3. RESULTS AND DISCUSSION

3.1. Synthesis and characterization of PTS

PTS was used in micelles production taking into account its self-emulsifying properties [143]. Moreover, PTS presents the ability for the solubilization of hydrophobic compounds [144, 145], and as a PEG derivative, also provides stealth to NPs, avoiding its early degradation and increasing its circulating half-life [151]. This compound was synthetized by conjugating PEG 600 to α-tocopherol, using sebacoyl dichloride [144]. The process was executed under anhydrous conditions in dry ethyl acetate with TEA [144]. The dimers formed during synthesis were precipitated by an excess of methanol and, in order to isolate the final product, the solvent was evaporated and the residue diluted with water and lyophilized [144]. After synthesis, the purified PTS was characterized by different techniques, such as ^{1}H NMR, DLS, MALDI-TOF and FTIR. Comparing the ^{1}H NMR spectrum of the synthetized PTS with the spectrum of commercial PTS it can be deduced that these two compounds have the same peaks at the same chemical shift. These results indicated that these two compounds have the same structure, being equivalent compounds (figure 14).

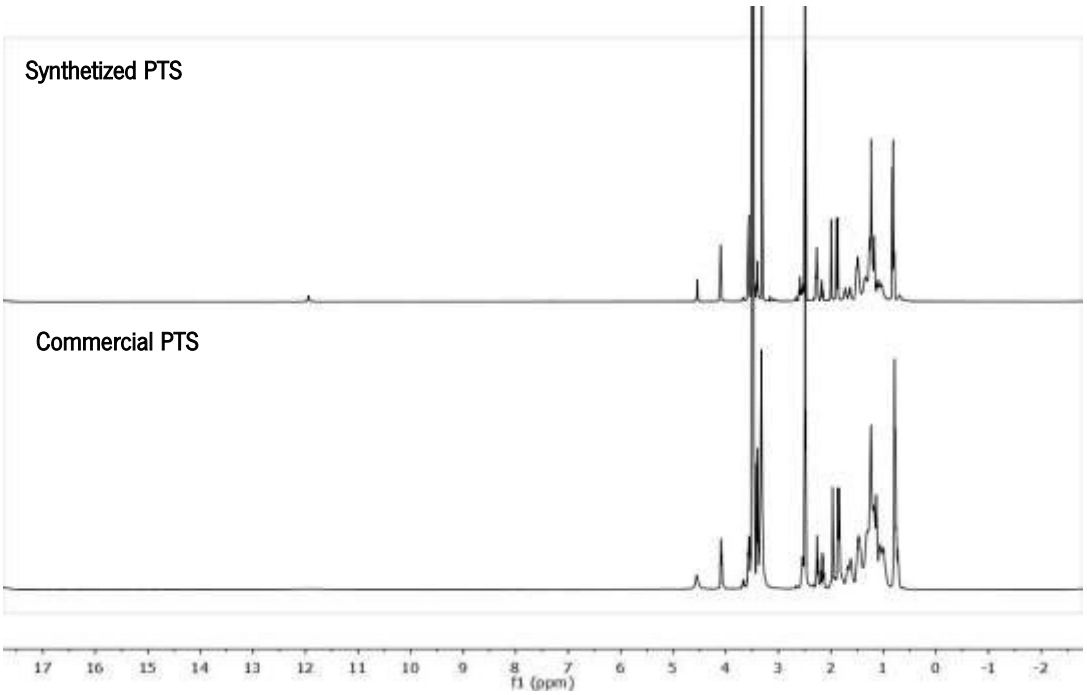

Figure 14 | ^{1}H NMR spectra of synthetized PTS and commercial PTS.

Taking into account the self-emulsifying properties of PTS, solutions of synthetized and commercial PTS at 5 mg/mL in water were prepared and analyzed by DLS. Table 3 shows the size and polydispersity index (PdI) values obtained for both compounds. The size and PdI of the NPs influence their interactions with the biological environment, the NPs' efficiency and its role as carriers [29, 34]. An adequate size range for NPs is between 10 and 150 nm [152, 153]. NPs with a size < 10 nm are prone to be easily cleared by kidney excretion and NPs with a size > 150 nm have a higher tendency of being cleared-off by MPS [153]. PdI is a parameter that represents the distribution of size populations and the numerical value of PdI ranges from 0.0 (for a uniform sample) to 1.0 (highly polydisperse sample with a broad size distribution or even several populations) [152, 154]. For samples of polymer-based NPs, PdI values of 0.2 and below are considered acceptable, indicating a homogenous population [152].

The solution prepared using the synthetized PTS showed better size and PdI values than the solution of commercial PTS (table 3). The size and PdI values of the micelles produced using synthetized PTS were within the optimal range described, demonstrating that this compound is promising for the micelles production. On the other hand, the solution of commercial PTS demonstrated the presence of NPs with larger size (approximately 360 nm) and a higher PdI value (approximately 0.3). Taking into account these results, the PTS synthetized in our laboratory was chosen for the development of PTS micelles.

Table 3 | Size (Z-average) and PdI values of solutions of synthetized PTS and commercial PTS at 5 mg/mL in water

Type of PTS	Z-average (d.nm)	PdI
Synthetized PTS	80.3	0.148
Commercial PTS	360.4	0.310

By MALDI-TOF analysis, it was observed that the average MW ($MW_{average}$) of the synthetized PTS is approximately 1283 Da, which is very similar to the MW previously described (1200 Da) [155].

The synthesis of PTS was also confirmed by FTIR analysis. Taking into account the structure of the PTS (figure 15), it was observed that its characteristic functional groups were present in the FTIR spectrum of the synthetized PTS (figure 16). The more relevant peak that indicates the ester formation is the C=O stretching at $\nu \approx 1700\ cm^{-1}$.

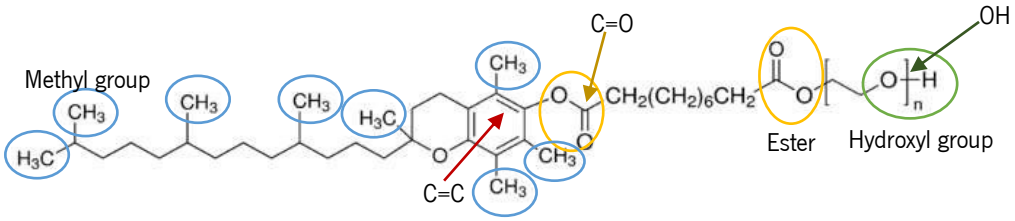

Figure 15 | Structure of PTS and its respective functional groups.

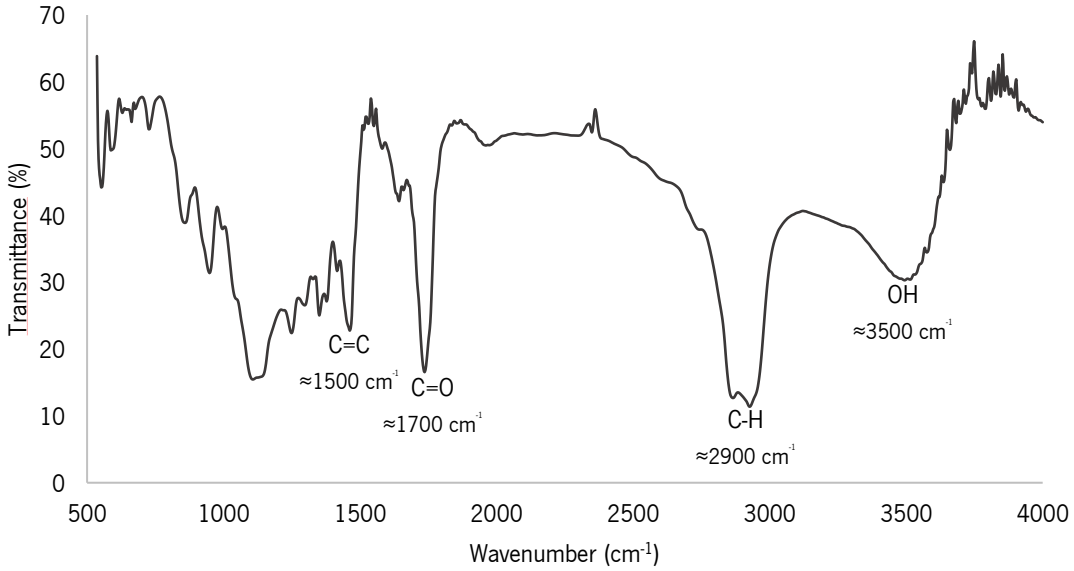

Figure 16 | FTIR spectrum of PTS.

In conclusion, all these results corroborated the already determined structure of PTS, indicating that the PTS produced in the laboratory was indeed equivalent to the commercial one.

In order to determine if the PTS could interfere in the quantification of MTX by the absorbance method, the absorbance spectrum of PTS was acquired (figure 17). It was verified that PTS presented a wavelength of maximum absorbance at 284 nm, different of the MTX (303 nm).

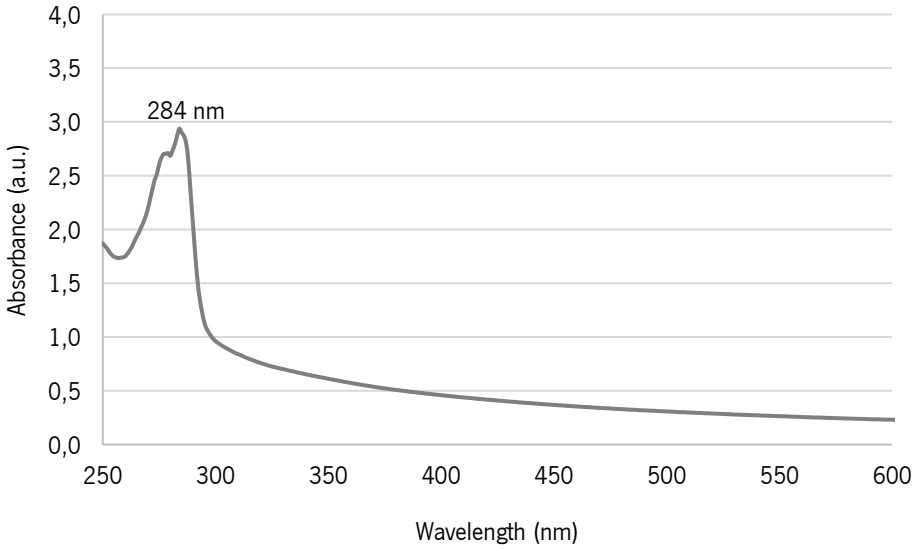

Figure 17 | Absorbance spectrum of PTS at 5 mg/mL in water.

3.2. Optimization of the PTS micelles production method and respective characterization of the developed micelles

The water-soluble PTS micelles were prepared through two different methods. In the auxiliary solvent method was used acetone, which was necessary as an auxiliary solvent for the solubilization of the lipophilic drug (MTX-OEt) in the initial formulation. In this way, it was necessary the evaporation of the acetone in order to produce suitable micelles for therapeutic applications. The second method used a high energy method (sonication) for the production of PTS micelles. The optimization of these two methods for micelles production was performed, testing different PTS concentrations and different temperatures of preparation.

Using the auxiliary solvent method, it was tested the evaporation of the acetone at 3 different temperatures (30 °C, 40 °C and 50 °C) using the rotary evaporator at 100 rpm. When the acetone evaporation was performed at 50 °C a considerable amount of water also evaporated, occurring loss of the sample. Thus, this evaporation temperature was not used in further steps. Several concentrations of PTS were tested (5, 10, 15, 20 and 25 mg/mL) using 30 °C and 40 °C in the evaporation step. Figure 18 shows the physicochemical properties obtained by DLS analysis and as it can be seen, all samples presented small size and PdI values, within the ideal size (10-150 nm) and PdI (≤ 0.2) range [152, 153].

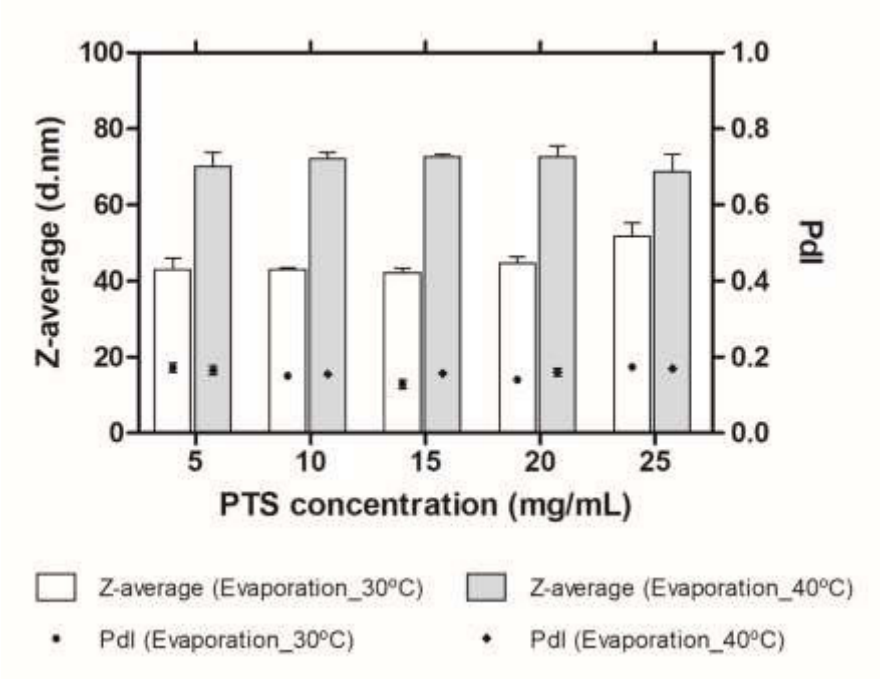

Figure 18 | Characterization in terms of size (Z-average) and PdI of PTS micelles produced by the auxiliary solvent method using the evaporation at 30 °C and 40 °C.

PTS micelles obtained after evaporation at 30 °C are smaller (40-50 nm) than micelles produced at 40 °C (65-75 nm). The optimal concentration of PTS chosen was 15 mg/mL, which showed a mean size of 42.4 ± 1.4 nm and a PdI value of 0.128 ± 0.016 for the samples prepared at 30 °C. All samples had zeta-potential values close to zero (0 ± 9 mV), indicating a neutral surface charge [156]. Neutral NPs are more suitable for IV therapeutic applications because they are associated with lower opsonization rates, reducing their clearance from the blood circulation [37, 41]. Another important point to take into account is the fact that all the produced PTS micelles remained stable for at least 8 weeks, maintaining their physicochemical properties unaltered. In conclusion, this method for PTS micelles production has great potential for further studies.

The production of PTS micelles through the sonication method was performed at two different temperatures (RT and 60 °C) applying 40 % of amplitude for 3 minutes. Several concentrations of PTS were tested (5, 10, 15, 20 and 25 mg/mL). Figure 19 shows that micelles produced at RT were considerably smaller and presented lower PdI values than micelles produced at 60 °C.

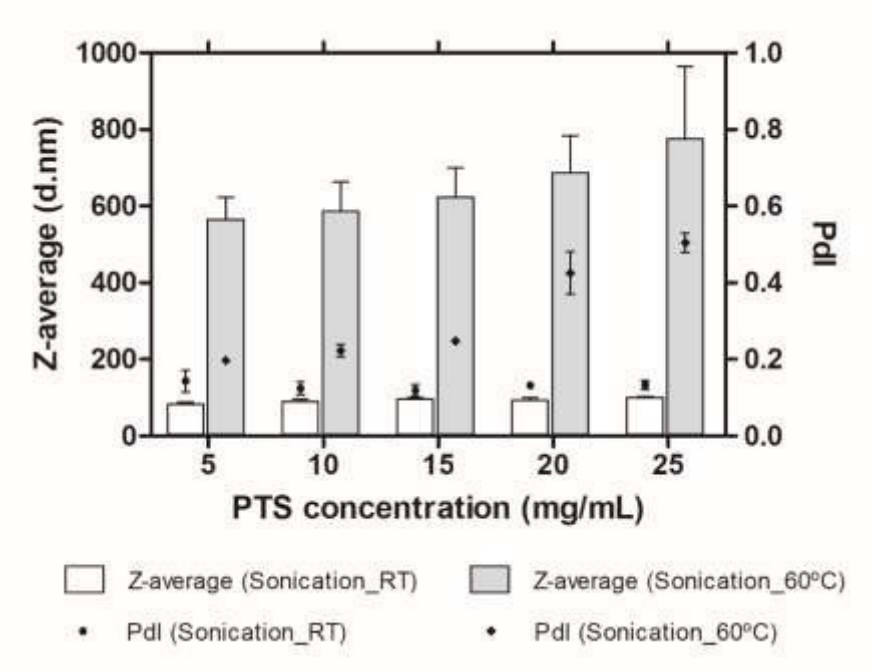

Figure 19 | Characterization in terms of size (Z-average) and PdI of PTS micelles produced by the sonication method at RT and 60 °C.

All samples prepared by sonication at RT demonstrated very similar size and PdI values, independently of the PTS concentration used. Micelles produced at RT also demonstrated high stability along time because their physicochemical characteristics remained unaltered for at least 8 weeks. The samples prepared at 60 °C showed to be less stable because their properties remained stable for only less than 4 weeks. The zeta-potential values obtained for all samples was also close to zero (0 ± 5 mV).

In conclusion, the PTS micelles produced using the auxiliary solvent method demonstrated better physicochemical characteristics than the micelles obtained by the sonication method. Micelles prepared using a solution at 15 mg/mL of PTS and through the auxiliary solvent method revealed to be promising NPs for an IV therapeutic application.

3.3. Biological characterization of the most promising PTS micelles

Cytotoxicity evaluation is of great importance, because the determination of this feature is a key factor to determine NPs potential and to enable its application [157]. As NPs for medical purposes usually involve intentional contact or administration, there is the need to understand and evaluate their effect on the body [157, 158]. Therefore, NPs for medical use must undergo rigorous testing in order to determine their biocompatibility when they enter the human organism and how they will

react [159]. The evaluation of the cytotoxicity of the most promising PTS micelles (prepared using 15 mg/mL of PTS through both described methods) was performed in normal human skin fibroblasts (BJ5ta cell line), represented below in figure 20.

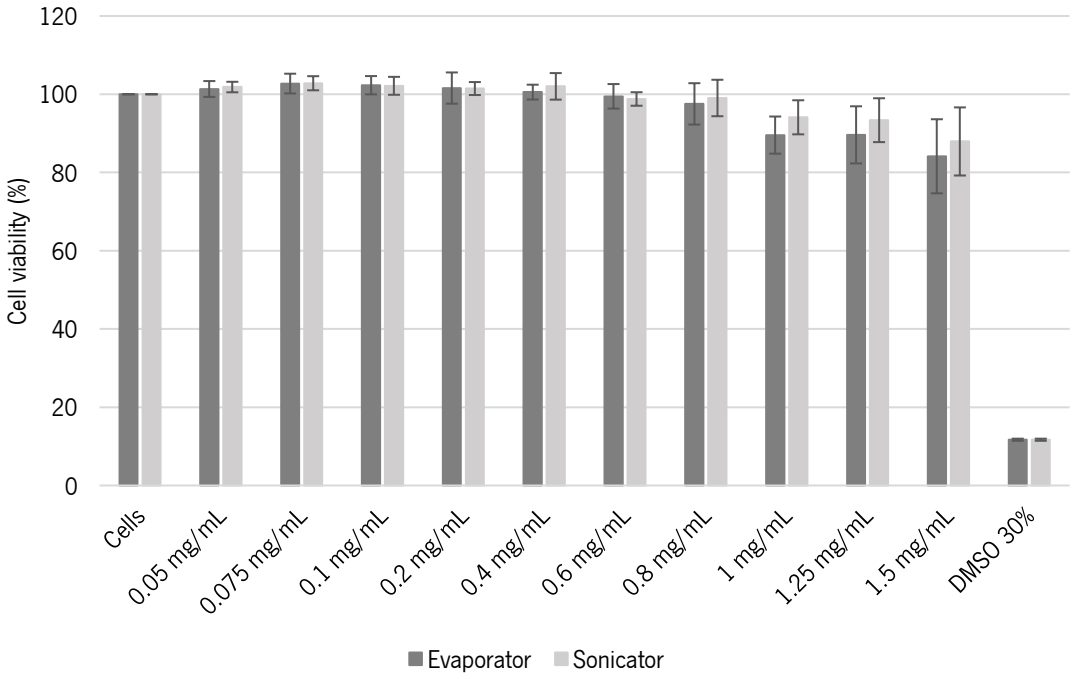

Figure 20 | BJ5ta cell line viability after 72 hours of contact with different concentrations of PTS micelles obtained using the auxiliary solvent method and the sonication method, compared with cells (negative control) and cells incubated with 30 % of DMSO (death control), determined by MTS assay. Values are the mean ± standard deviation (SD) of 3 independent experiments.

Figure 20 shows that cells incubated with PTS micelles obtained through both methods (auxiliary solvent and sonication) revealed very similar values of cell viability. Until 1 mg/mL, the PTS micelles did not induce loss of cell viability even after 72 hours of contact. For higher concentrations of PTS micelles, it was observed that the micelles induced very low cytotoxicity levels (< 20 %), being the cell viability superior than 80 %. This results indicated that the developed PTS micelles were not harmful to normal cells and consequently were safe to be used in further studies.

3.4. Development of PTS micelles loaded with the hydrophobic MTX derivative, MTX-OEt

3.4.1. Characterization of MTX-OEt

The new hydrophobic MTX derivative (MTX-OEt) was characterized by ^{1}H NMR spectroscopy and MALDI-TOF analysis. ^{1}H NMR spectrum of MTX-OEt showed the characteristic peaks of the MTX and also the peaks of the formed ester (ethyl group) (**k** and **j**), which confirmed the conjugation. The purity of the compound was evaluated by the absence of peaks that are not related to the conjugate (figure 21).

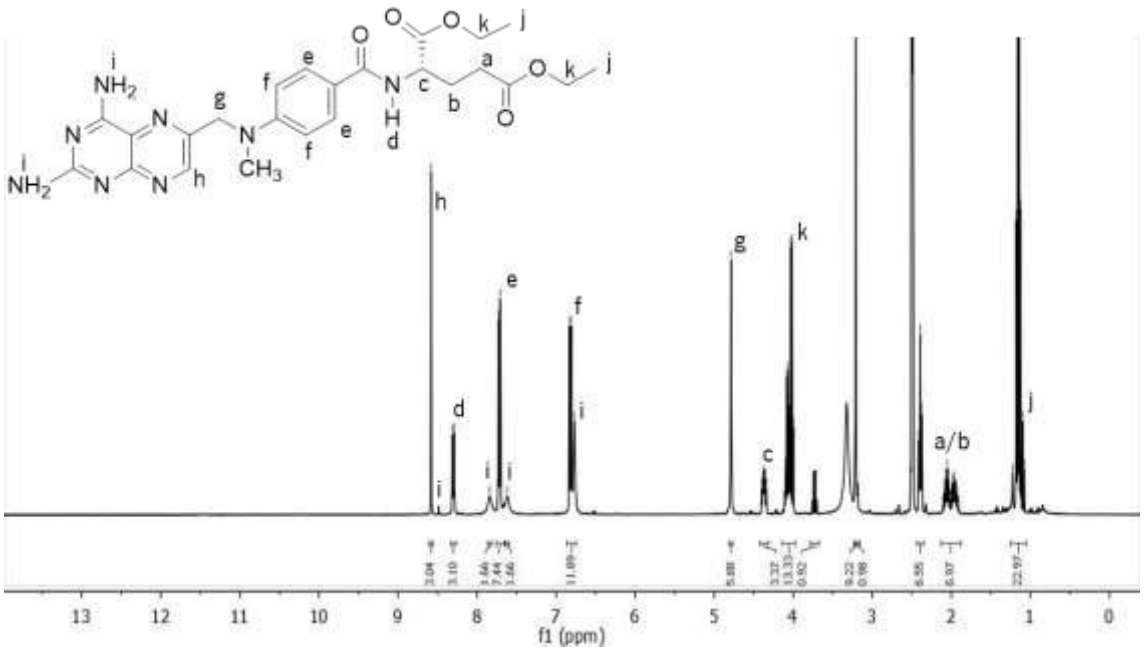

Figure 21 | ^{1}H NMR spectrum of MTX-OEt in DMSO-d_6. The peaks labeled in lowercase letters correspond to the protons indicated in the structure of MTX-OEt.

By MALDI-TOF analysis, it was possible to obtain the $MW_{average}$ of MTX-OEt (510.24 Da) which was similar to the calculated MW (510.55 Da). This result further confirmed the purity and the MW of MTX-OEt (figure 22).

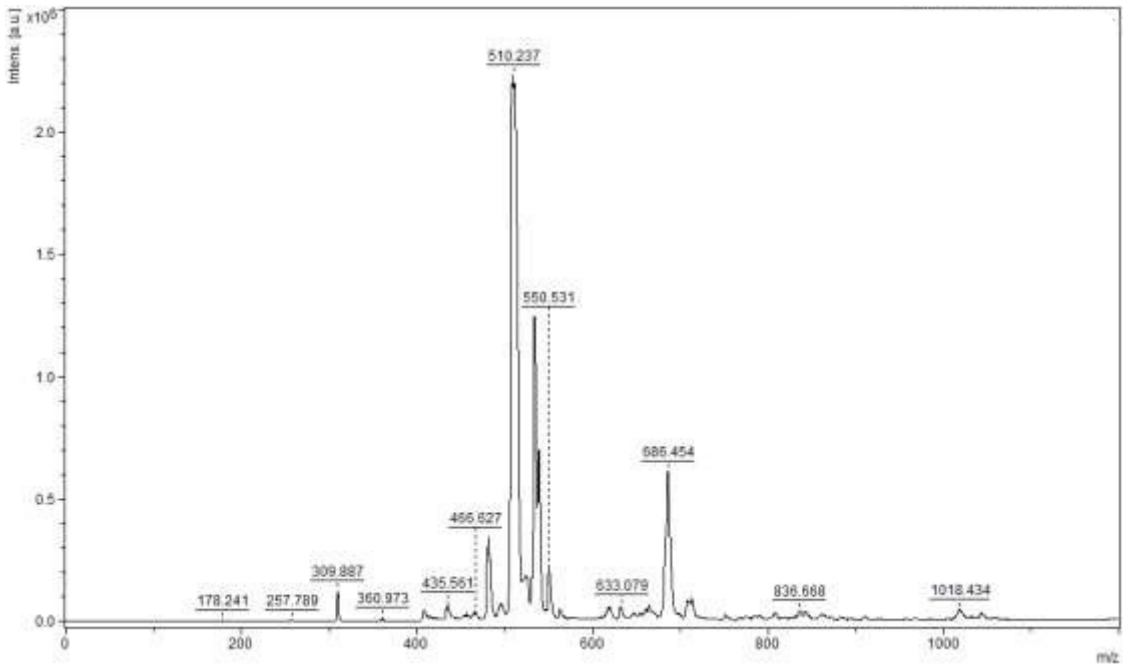

Figure 22 | MALDI-TOF mass spectrum of MTX-OEt, acquired in linear positive mode.

The absorbance spectrum of MTX-OEt was performed in order to verify if this MTX derivative presented the same wavelength of maximum absorbance than MTX, which is used for the drug quantification. The absorbance spectra of both compounds revealed to be very similar, indicating that the MTX-OEt can be quantified by absorbance using the same wavelength (303 nm) used for the quantification of the MTX (figure 23).

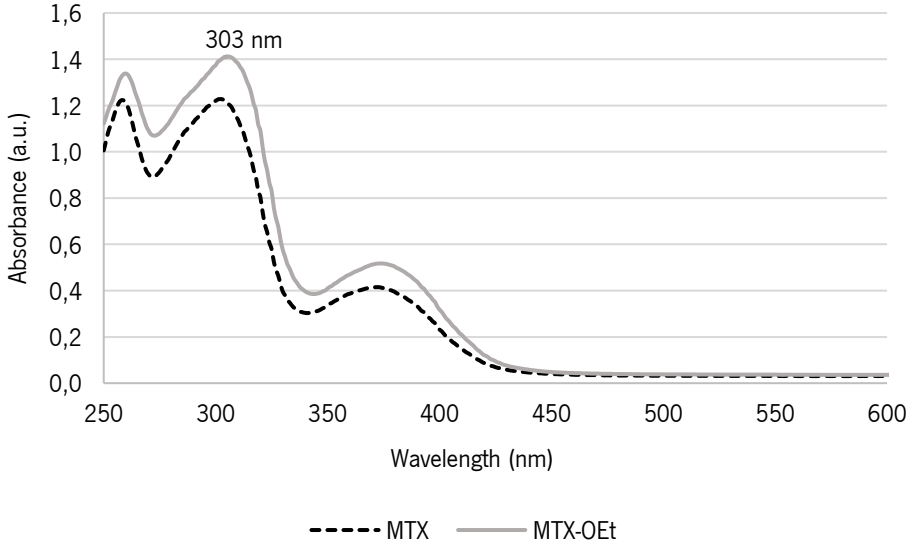

Figure 23 | Absorbance spectra of MTX and MTX-OEt, both at 0.1 mM of MTX.

3.4.2. Preparation and characterization of PTS micelles loaded with MTX-OEt

The next step of the work was the encapsulation of the MTX-OEt in the developed PTS micelles. This hydrophobic MTX derivative was the chosen drug due to its hydrophobic nature, which is ideal for its encapsulation in the hydrophobic core of the micelles.

Micelles loaded with MTX-OEt were produced using the two previously described methods (auxiliary solvent and sonication) and several PTS/MTX-OEt mass ratios were tested. In the auxiliary solvent method, the two compounds were weighted in different PTS/MTX-OEt mass ratios (3:1, 6:1 and 8:1), maintaining the PTS concentration at 15 mg/mL. Then, acetone and water were added and the samples were placed in the rotary evaporator at 30 °C, 100 rpm for 30 minutes. Table 4 shows the results of the physicochemical characterization of the micelles loaded with MTX-OEt.

Table 4 | Physicochemical characterization of PTS micelles loaded with MTX-OEt prepared through auxiliary solvent method (evaporation at 30 °C) and using the PTS/MTX-OEt mass ratios of 3:1, 6:1, 8:1. Values represent the mean ± SD of 3 independent experiments

PTS/MTX-OEt Mass ratio	Z-average (d.nm)	PdI	Zeta-potential (mV)
3:1	530.5 ± 200.6	0.631 ± 0.072	8.20 ± 0.01
6:1	60.4 ± 1.3	0.301 ± 0.040	4.24 ± 0.59
8:1	56.9 ± 0.7	0.292 ± 0.027	6.89 ± 0.10

The sample prepared using the 3:1 ratio revealed high values of size and PdI, meaning that the sample is heterogeneous and presents large micelles that are not suitable for IV therapeutic applications. The results obtained for the samples prepared using 6:1 and 8:1 mass ratios were very similar. The micelles size was approximately 60 nm, which is within the optimal size range (10-150 nm) [152, 153]. The PdI values were higher than 0.2, however this value is still described as acceptable for therapeutic applications [160]. It is of importance to notice that the 8:1 mass ratio remained stable for a longer period of time and showed less precipitation than the 6:1 mass ratio. So, further tests were done with the PTS/MTX-OEt mass ratio of 8:1. NPs that present zeta-potential values between −10 and +10 mV are considered neutral NPs [156]. In this way, all the obtained micelles loaded with MTX-OEt presented neutral surface charge.

Although the empty PTS micelles demonstrated to be stable even after 8 weeks of storage, the same micelles loaded with MTX-OEt revealed precipitation a few days after preparation. This

precipitation occurred when the free drug was not separated from the micelles, thus it was very important to select a suitable separation method in order to provide stable micelles.

Using the sonication method, PTS and MTX-OEt were also weighed but only water was added and then these samples were subjected to sonication at an amplitude of 40 % for 3 min. PTS concentration was maintained at 15 mg/mL and three PTS/MTX-OEt ratios (w/w) were tested (6:1, 8:1 and 10:1). Also, two different temperatures were tested (RT and 60 °C) and although the best results obtained for the empty PTS micelles were at RT, for PTS micelles loaded with MTX-OEt, the sonication at this temperature was not successful. Figure 24 shows photographs of the samples after sonication process and it is visible that in the case of the samples prepared at RT (figure 24 A, B and C) was not obtained a limpid solution, due to the presence of precipitated MTX-OEt. MTX-OEt was not totally solubilized in the solution, which indicated that the micelles were not correctly formed, not occurring the entrapment of the MTX-OEt and consequently not occurring its solubilization in water.

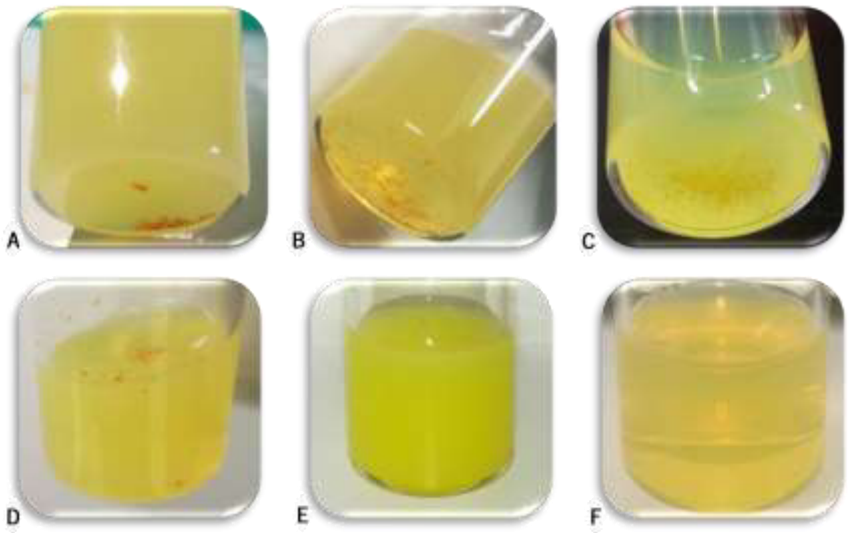

Figure 24 | Photographs of the samples prepared by sonication method at RT and 60 °C, using 3 different PTS/MTX-OEt mass ratios (6:1; 8:1; 10:1). Images A, B and C correspond to the samples prepared by sonication method at RT and using the 6:1; 8:1 and 10:1 mass ratios, respectively. Images D, E and F correspond to the samples prepared by sonication method at 60 °C and using the 6:1; 8:1 and 10:1 mass ratios, respectively.

Taking into account the appearance of the samples after sonication at 60 °C (figure 24 D, E and F), it was possible to infer that using the mass ratio of 6:1 did not occur the successful formation of the micelles. However, the production of PTS micelles loaded with MTX-OEt using the mass

ratios of 8:1 and 10:1 was possible through the sonication at 60 °C. These two samples were analyzed by DLS and the results obtained are presented in table 5.

Table 5 | Physicochemical characterization of PTS micelles loaded with MTX-OEt prepared through sonication at 60 °C and using the PTS/MTX-OEt mass ratios of 8:1 and 10:1. Values are the mean ± SD of 3 independent experiments

PTS/MTX-OEt Mass ratio	Z-average (d.nm)	PdI	Zeta-potential (mV)
8:1	87.3 ± 3.1	0.127 ± 0.011	12.80 ± 0.71
10:1	99.4 ± 1.5	0.098 ± 0.009	15.65 ± 0.78

Analyzing the results obtained, it can be concluded that both samples are very similar and present suitable characteristics for IV therapeutic applications (homogeneous population and small size). Micelles prepared using the 10:1 mass ratio demonstrated to be slightly better (PdI< 0.1). The zeta-potential values of the samples were > 10 mV, being these micelles considered slightly cationic [156]. This cationic surface can induce more permeation across the membranes (that are negatively charged) [156]. Also, an increased phagocytosis, higher rate of cell uptake, higher nonspecific internalization rate and short blood circulation half-life can occur in this case [34, 37, 39]. However, these micelles are PEGylated which gives them stabilized properties and stealth features [28, 43], reducing their quick clearance and degradation.

For both samples (PTS/MTX-OEt mass ratio of 8:1 and 10:1), before the separation of the free drug, was observed precipitation after the overnight storage. Moreover, the results obtained in these conditions were poorly reproducible because sometimes the MTX-OEt did not dissolve completely after the sonication. In this way, comparing the results obtained for the micelles produced through the two production methods it was visible that the auxiliary solvent method was more reproducible and resulted in more stable micelles.

The next step of the work was the separation of the free drug from the micelles. Micelles loaded with MTX-OEt were produced through the two described production methods (auxiliary solvent and sonication) using the PTS/MTX-OEt mass ratio of 8:1. Several approaches were performed for the separation of the free drug, such as dialysis tubes, desalting columns, amicons, ultrafiltration system and also the tangential filtration. Tangential filtration was the only approach that allowed an effective separation of the free drug, being possible the quantification of the encapsulated MTX-

OEt and the determination of the EE. Beyond the MTX-OEt quantification, the samples after the tangential filtration were also analyzed in terms of size and PdI (table 6).

Table 6 | Physicochemical characteristics (size (Z-average) and PdI values)), concentration of encapsulated MTX-OEt and the EE of PTS micelles loaded with MTX-OEt after tangential filtration. Values are the mean ± SD of 2 independent experiments

Method	Compensation solution	Z-average (d.nm)	PdI	MTX-OEt Concentration* (mg/mL)	EE (%)
Auxiliary solvent	Water	68.7 ± 23.7	0.227 ± 0.045	0.152 ± 0.035	8.1 ± 1.9
	PBS	104.4 ± 3.9	0.162 ± 0.024	0.136 ± 0.023	7.3 ± 1.2
Sonication	Water	41.5 ± 14.1	0.332 ± 0.296	0.102 ± 0.013	5.5 ± 0.7

*Determined by absorbance measurements at 303 nm

The samples obtained through the auxiliary solvent and the sonication methods were placed in the tangential filtration system using water as compensation solution, which is the same solvent used for their production. The samples prepared by sonication showed smaller size values but higher PdI than the samples prepared using the auxiliary solvent method. Moreover, the EE of the micelles produced by sonication was the lowest. In this way, the micelles prepared through the auxiliary solvent method demonstrated to be more promising for therapeutic applications. These micelles presented smaller PdI values, being more homogenous, and also presented more encapsulated MTX-OEt. Taking into account the desired application of these micelles, the tangential filtration was also tested using PBS as compensation solution. This process was performed for the separation of the free drug but also allowed the exchange of the solvent to a buffer solution. The obtained micelles demonstrated suitable physicochemical properties (small size and PdI values) and a similar concentration of encapsulated MTX-OEt. The zeta-potential value of this sample was < -10 mV, indicating that these micelles presented neutral surface charge [156].

The stability of the samples after the tangential filtration process was also evaluated and it was observed that the micelles obtained by the auxiliary solvent method demonstrated high stability through a period of time of at least 8 weeks. In the case of micelles obtained from the sonication method, they lost their stability after only 4 weeks of storage.

In conclusion, the selected method for the production of PTS micelles loaded with MTX-OEt was the auxiliary solvent method at 30 °C, using PTS at 15 mg/mL and a PTS/MTX-OEt mass ratio of 8:1. Using these conditions, it was possible to obtain homogeneous populations of small and stable micelles with a higher drug EE. Furthermore, the whole process of production demonstrated to be more reproducible. In this way, further characterization processes were performed with these samples after the separation of free drug using the tangential filtration.

3.4.3. Biological effect of PTS micelles loaded with MTX-OEt

MTX is one of the most widely used drugs in cancer therapy [136, 140] also being one of the most effective [135]. However, MTX therapy presents some limitations such as high toxicity in normal cells due to its low specificity and short plasma half-life [136, 140]. Therefore, the use of DDS for MTX delivery to the tumor site appears as a promising approach [139, 140] that can reduce the side effects of MTX and improve its therapeutic efficacy [138]. NPs are able to protect the drug in the systemic circulation and can deliver the drug at a controlled and sustained rate [161-163]. Thus, the NPs can reduce the therapeutic toxicity and enhance drug bioavailability [161-163]. In sum, NPs are able to improve the pharmacokinetic and pharmacodynamic properties of pharmacological compounds [161, 163].

In order to compare the biological effect of the micelles loaded with MTX-OEt with free MTX-OEt at the same concentration, the cell viability was assessed on cancer cells (Caco-2 cell line). Caco-2 cells were incubated with micelles loaded with MTX-OEt, empty micelles, MTX-OEt and unmodified MTX that was used as a control. The results obtained are presented in figure 25.

Figure 25 shows that the micelles loaded with MTX-OEt, free MTX-OEt and unmodified MTX revealed very similar values of cell viability. These results support two important points: the hydrophobic derivative of MTX presents the same anticancer effect than the unmodified drug and the developed micelles present the important ability to promote an effective release of the drug *in vitro*. As the modified MTX (MTX-OEt) and the commercial MTX demonstrated a similar behavior, it can be concluded that the modification did not affect the interaction of the drug with the cells. Also, the incubation of Caco-2 cells with empty micelles did not induce cytotoxicity even after 72 hours of incubation, as expected.

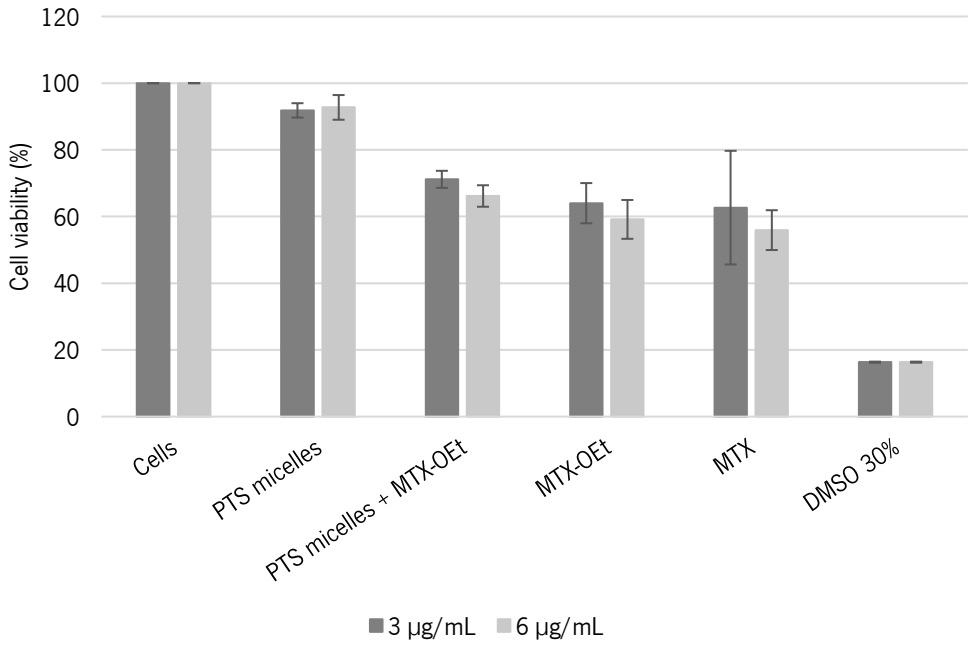

Figure 25 | Caco-2 cell line viability after 72 hours of contact with micelles obtained by auxiliary solvent method, compared with cells (negative control) and cells incubated with 30 % of DMSO (death control), determined by MTS assay. Values are the mean ± SD of 3 independent experiments.

4. CONCLUSIONS

The results obtained in this work showed that the PTS production in the laboratory was successfully achieved. The characterization by NMR, FTIR and MALDI-TOF demonstrated that the synthetized PTS presents the same structure as the commercial one. Furthermore, the synthetized PTS enabled the formation of micelles with the best physicochemical characteristics, being also a low-cost way of obtaining the compound.

Using two different methods, several optimizations were performed in order to obtain the most promising PTS micelles. The optimal production method was reached, which was based on the auxiliary solvent method with evaporation at 30 °C, an agitation speed of 100 rpm and a PTS concentration of 15 mg/mL. These PTS micelles were then tested in human skin fibroblasts cell line and the results showed that these micelles did not induce cytotoxicity in normal human cells, even after 72 hours.

In order to encapsulate MTX in these PEGylated micelles it was used a hydrophobic derivative of MTX (MTX-OEt). The characterization of this new compound allowed the confirmation of its structure and purity. Several mass ratios of PTS/MTX-OEt were tested and the best results were obtained when the 8:1 (w/w) ratio was used. These micelles showed a small size and low PdI values, being promising NPs for IV therapeutic applications. Moreover, these PEGylated micelles loaded with MTX-OEt revealed the expected biological effect against cancer cells (Caco-2 cells).

In conclusion, the results obtained in this work highlight the development of PTS micelles as suitable therapeutic DDS, which have potential for further research studies. In the future, one of the main objectives is the incorporation of a targeting ligand in the PTS micelles loaded with MTX-OEt in order to allow a specific delivery of the drug to the cancer cell population. With these final PEGylated micelles it is also expected the performance of *in vivo* experiments. Similarly, using the optimized micelle formulation it can also be tested the incorporation of other pharmacological compounds, widening its therapeutic range to different clinical applications.

CHAPTER IV

FA-tagged liposomes for delivery of a methotrexate derivative

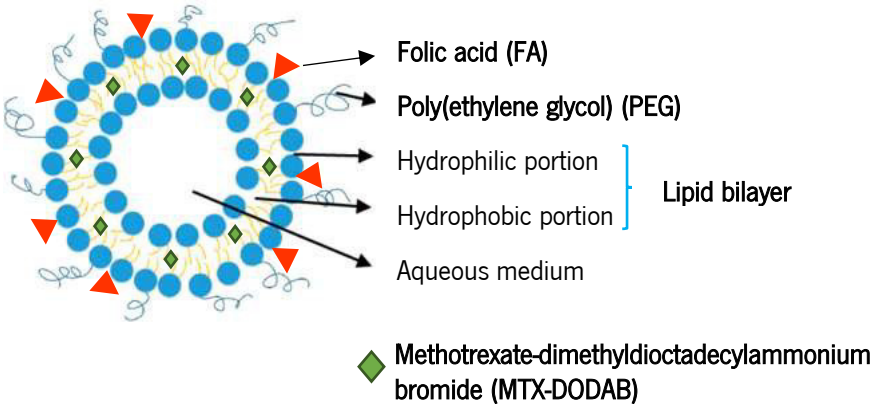

Chapter IV – FA-TAGGED LIPOSOMES FOR DELIVERY OF A METHOTREXATE DERIVATIVE

1. FRAMEWORK

In this chapter is described the development of FA-tagged liposomes loaded with another hydrophobic MTX derivative, MTX-DODAB, produced in our laboratory. For the liposomes preparation was used a formulation previously developed by colleagues of the laboratory, which results in the production of FA-tagged liposomes.

The liposomes were prepared by the ethanol injection method and several optimizations were performed in order to produce liposomes with suitable characteristics for IV therapeutic applications. Then, their physicochemical and biological characterizations were performed.

In sum, it is expected that the developed liposomes can improve the efficacy and safety of MTX, overcoming the several limitations associated with conventional cancer therapy.

2. MATERIALS AND METHODS

2.1. Reagents and Equipment

2.1.1. Reagents

For liposomes preparation were used: SP-DS3-FA peptide, 1,2-distearoyl-sn-glycero-3-phosphoethanolamine-*N*-[methoxy(polyethylene glycol)-2000] (DSPE-mPEG 2000), 1,2-dioleoyl-sn-glycero-3-phosphoethanolamine (DOPE), cholesterol, MTX-DODAB, ethanol, PBS and ultrapure water. MTX and DODAB were purchased from TCI Chemicals (Belgium). DOPE and DSPE–mPEG 2000 were purchased from Lipoid GmbH (Germany). SP-DS3-FA peptide was purchased from CSBio (CA, USA). Cholesterol was obtained from Sigma-Aldrich (USA). Ethanol was acquired from Fisher Scientific (UK). PBS was purchased from Biochrom GmbH (Germany) and ultrapure water was obtained from a Milli-Q Water Purification System (Germany).

For the characterization of the developed liposomes through ^{1}H NMR spectroscopy, DMSO-d_6 (Cortecnet, France) was used as a solvent. Pyridine (Sigma-Aldrich, USA) as an internal standard was added to NMR tube for drug quantification.

Liposomes for the cellular tests were filtered under sterile conditions using 0.22 μm PES filter, purchased from Merck Millipore (Ireland). Caco-2 cell line from ATCC (UK) was used in all cellular tests. T75 flasks and 96-well tissue culture polystyrene plates were purchased from SPL Life Sciences (Korea). Culture medium and supplements were purchased from Sigma-Aldrich (USA). The cell viability tests were done using MTS assay, which was purchased from Promega (USA).

2.1.2. Equipment

For the separation of free drug from the liposomes, PD-10 sephadex desalting columns (MWCO= 5 kDa) were used.

DLS analysis was performed in a Malvern Zetasizer Nano ZS from Malvern Panalytical (UK). Nanoparticle tracking analysis (NTA) measurements were performed using a NanoSight NS500 instrument, from Malvern Panalytical (UK). All absorbance measurements were conducted at a wavelength of 303 nm using a Synergy Mx Multi-Mode Reader from BioTek (USA). The samples analyzed through NMR spectroscopy were previously lyophilized using the Lyophilizer FreeZone 2.5, purchased from Labconco® (USA). ^{1}H NMR spectroscopy was executed in a Bruker Avance III 400 (Bruker Daltonics GmbH).

All cellular tests were done in a ScanLaf Mars laminar flow chamber from Labogene (Denmark) and the cell culture was maintained in Thermo Heraeus HeraCell 150 CO_2 Incubator from Hofstra Group (USA).

2.2. Production of the methotrexate derivatives

2.2.1. MTX disodium salt (MTX-Na)

Commercial MTX was dissolved in water and 2 equivalents of NaOH were added to the solution. The solution was vortexed until total MTX solubilization and the pH was corrected until pH=7 using a solution of HCl 5 M. Then, the solution was freeze-dried to obtain the MTX-Na as an orange solid.

2.2.2. MTX-DODAB complex

For MTX-DODAB complex production, MTX-Na and DODAB (1:2 molar ratio) were dissolved in a mixture of water and ethanol at a 50/50 (v/v) ratio. The reaction was performed for 70 minutes at 70 °C and under a magnetic stirring of 700 rpm. Afterwards, the solution was filtered by gravity (Prat Dumas, France) and dried overnight, obtaining MTX-DODAB complex as a yellow solid. Several optimizations were performed in the MTX-DODAB complex production method in order to develop a green method and to obtain the best yield of reaction. Initially, the organic solvent used was chloroform, however, later it was substituted for ethanol. Also, different quantities of both compounds were tested, maintaining the molar ratio. The complex characterization was performed by ^{1}H NMR and the yield was calculated using equation 3, being DODAB the limiting reagent and η the yield of the reaction expressed in percentage.

$$\eta\,(\%) = \frac{nº\ of\ moles\ of\ MTX - DODAB\ complex}{nº\ of\ moles\ of\ limiting\ reagent} * 100$$

Equation 3 | Determination of the yield of the reaction for MTX-DODAB complex production.

The ^{1}H NMR spectroscopy of MTX-DODAB was performed using the same conditions used for the characterization of MTX-OEt.

The absorbance spectrum of MTX-DODAB was performed in order to verify if the wavelength of maximum absorbance is the same as the unmodified MTX (λ= 303 nm).

2.3. Production and characterization of FA-tagged liposomes loaded with MTX-DODAB

2.3.1. Preparation of liposomes by ethanol injection method

Ethanol injection method is based on the injection drop by drop of the organic phase (ethanol) into the aqueous phase (water or PBS) using a syringe. For all formulations, the ratio (v/v) between organic and aqueous phases was set to 50/50 %. In the organic phase (ethanol) were dissolved DOPE/Cholesterol/DSPE-mPEG 2000 in a 54/36/10 molar ratio (at a final DOPE concentration of 9 and 18 mM), the drug (MTX-DODAB) and also FA-peptide. After the solubilization of all components, the ethanol phase was injected into the aqueous phase through a syringe. This process was conducted at 70 °C and under magnetic stirring at 500 rpm for 10 minutes, leading to the ethanol evaporation and the liposomes production.

The free FA-peptide and the free drug that were not incorporated into liposomes were removed from the liposomal formulations through the desalting columns (MWCO= 5 kDa). Finally, the liposomes were filtered under sterile conditions using 0.22 μm PES filter.

2.3.2. Liposomes characterization

2.3.2.1. Physicochemical characterization of liposomes

The liposomes were characterized through two different techniques, DLS and NTA. The average size, PdI and zeta-potential values were obtained using the first technique where the liposomes dispersed in PBS buffer were analyzed at pH 7.4 and at 25 °C. The viscosity and refractive index values used were 0.8616 cP (PBS) and 1.440, respectively. Lipid concentration was held constant at 600 μM. Liposomal formulations were stored at 4 °C for a period of 16 weeks and their physicochemical parameters were periodically measured in order to study NPs stability.

The concentration of the liposomes as well as their size distribution were obtained by NTA. NTA measurements allowed the visualization and tracking of the Brownian motion of laser-illuminated particles in suspension. The samples were diluted with water, injected into the system and analyzed at RT. Then, the video sequence of each sample was captured over 60 seconds with manual shutter and gain adjustments, providing important parameters in liposomes' characterization, namely the concentration of liposomes and its size distribution.

2.3.2.2. Determination of the encapsulation efficiency

^{1}H NMR spectroscopy of the liposomes loaded with MTX-DODAB was performed using DMSO-d_6. Pyridine was used as an internal standard for drug quantification and the chemical shifts were reported as δ (ppm). Taking into account the values of the integration of one aromatic peak of MTX (δ_H= 6.80 ppm), the calculations of the drug concentration encapsulated in the liposomes were performed. Using this drug concentration obtained by NMR spectroscopy, the EE was calculated using equation 1 (Chapter III), previously described in PTS micelles characterization.

As the components of the liposomal formulations showed an interference in the quantification of MTX by absorbance, in this case, the free drug was quantified measuring the absorbance at λ= 303 nm, after separation from the liposomes phase. A calibration curve was performed and the free MTX concentration was calculated. The EE was determined using the equation 4, where $[drug]_{initial}$ is the total concentration of drug added to the initial formulation and $[drug]_{free}$ is the total concentration of drug that was not encapsulated in the liposomes.

$$Encapsulation\ efficiency\ (\%) = \frac{[drug]_{initial} - [drug]_{free}}{[drug]_{initial}} * 100$$

Equation 4 | Determination of liposomes EE.

2.4. Evaluation of the biological effect of the developed liposomes loaded with MTX-DODAB

2.4.1. Cells and culture conditions

The biological effect of liposomes loaded with MTX-DODAB was analyzed using Caco-2 adherent cell line. These cells were grown in T75 flasks and maintained under a humidified atmosphere of 5 % CO_2 in air and at 37 °C. Caco-2 cell line required specific medium conditions, which are detailed in table 2 (Chapter III).

2.4.2. Cell Viability Assay

Cell viability was tested using the Cell Proliferation MTS assay, the same method described for the biological characterization of the PTS micelles. Caco-2 cells were seeded in 96-well tissue culture polystyrene plates at a density of 1×10^4 cells/well and incubated overnight to promote cell adhesion. Then, the cells were incubated with two different concentrations (10 and 25 μg/mL) of

free MTX and with liposomes loaded with the same concentrations of MTX, as well as with the respective controls of empty liposomes, for 72 hours at 37 °C. Subsequently a MTS mixture was added to each well and the cells were incubated for 4 hours at 37 °C. Finally, the absorbance of the formazan product was read at 490 nm. Cell viability was calculated using equation 2 previously described in Chapter III and expressed as a percentage relative to the negative control, the untreated cells.

3. RESULTS AND DISCUSSION

3.1. Synthesis and characterization of the hydrophobic MTX derivative, MTX-DODAB

In order to synthetize the MTX-DODAB complex, it was necessary the production of MTX-Na, which reactional scheme can be visualized below in figure 26.

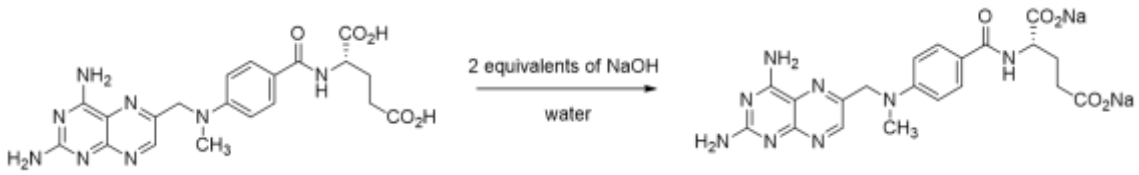

Figure 26 | Conversion of MTX to MTX-Na, with the addition of 2 equivalents of NaOH.

MTX-DODAB complex was formed by an ionic interaction between the MTX that presents a negative charge (carboxylic groups) and the cationic lipid DODAB. Since DODAB has a quaternary amine, it is impossible the formation of a covalent bond with other molecules. In this way, the most favorable interaction to occur with this molecule is ionic. The reactional scheme for the complex formation is represented in figure 27.

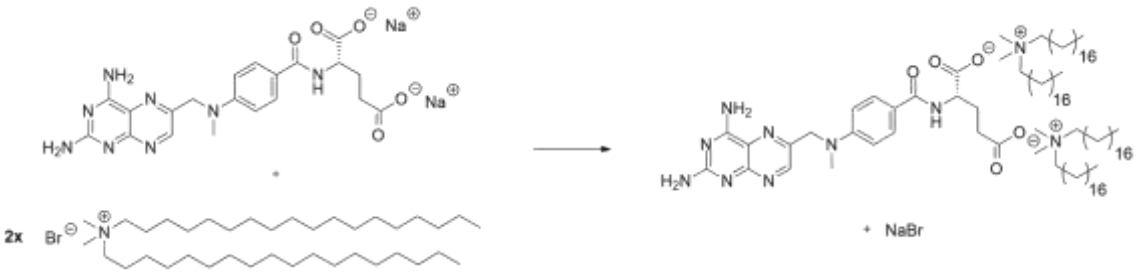

Figure 27 | Reactional scheme of MTX-DODAB formation.

During the MTX-DODAB synthesis the ethanol was evaporated and a yellow solid precipitated in the aqueous medium. After the product isolation and identification, the hydrophobic MTX derivative was obtained. The yield of MTX-DODAB production was $\eta = 45.5$ %. The complex was then analyzed by ^{1}H NMR (figure 28) in order to confirm the MTX-DODAB complex structure and purity.

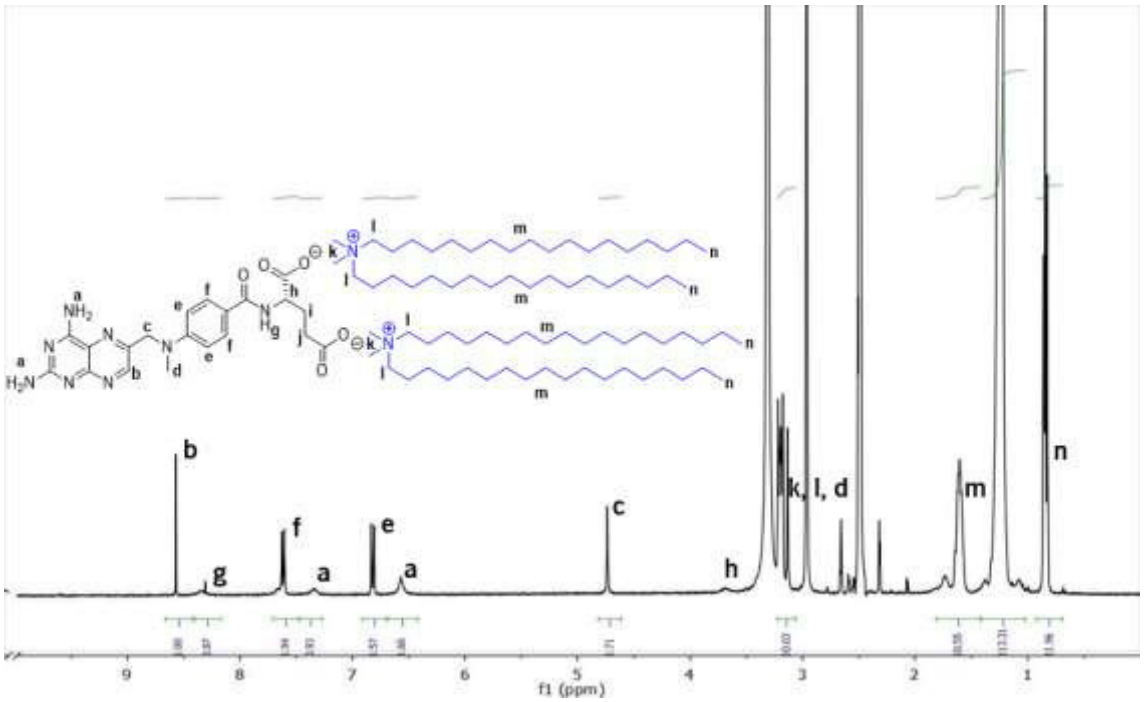

Figure 28 | ^{1}H NMR spectrum of MTX-DODAB complex. The peaks labeled in bold lowercase letters correspond to the protons indicated in the structure of MTX-DODAB complex.

The ^{1}H NMR spectrum of the MTX-DODAB complex (figure 28) showed a chemical shift of the peaks that correspond to the protons in the proximity of the ionic interaction (**g** to **j**). By the comparison of the integration between protons **b** and protons **n**, the ^{1}H NMR spectroscopy also allowed to determine that there were 2 molecules of DODAB for 1 molecule of MTX. The absence of free initial reactants proved the purity of the complex.

Additionally, the absorbance spectrum of the MTX-DODAB complex was also performed (figure 29).

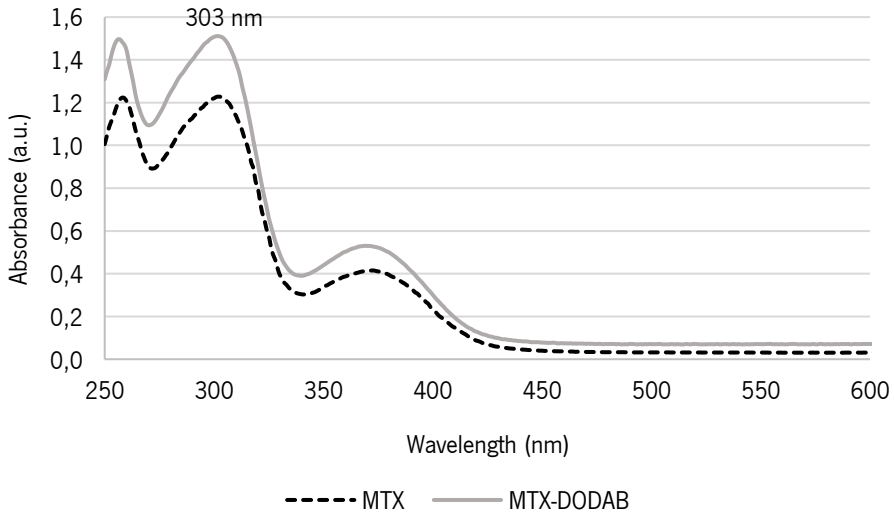

Figure 29 | Absorbance spectra of MTX and MTX-DODAB complex, both at 0.1 mM of MTX.

The absorbance spectrum of the MTX-DODAB complex revealed to be very similar to the unmodified MTX spectrum (figure 29), indicating that DODAB did not interfere in the quantification of MTX through the absorbance.

3.2. Preparation and characterization of liposomes loaded with MTX-DODAB

The formulation used for the production of liposomes was the same previously optimized by a colleague of our laboratory [164-167]. The physicochemical and biological characterizations of empty liposomes were already performed and published. According to Nogueira *et al.,* 2015, the liposomal formulation exhibited a narrow size distribution (PdI< 0.1), small size (< 150 nm) and neutral surface charge [166]. The evaluation of the cytotoxicity demonstrated that the liposomal formulations, over a broad range of concentrations (up to 750 μg/mL), did not induce cytotoxicity in normal human cells (BJ5ta cell line) [166].

For liposomal formulations, a PdI value of 0.1 and below indicates monodispersity [168, 169]. Relatively to the size, it has been described that liposomes used for drug delivery should have a size lower than 300 nm [153]. Additionally, an optimal size range for NPs is between 100 and 200 nm, being large enough to avoid uptake in the liver and small enough to avoid filtration in the spleen, leading to a prolonged circulation time [170]. In this way, several optimizations were performed in the ethanol injection method in order to produce liposomes with suitable characteristics for the intended purpose. For that it was tested different agitation speeds, magnetic stirring bars and concentrations of DOPE (9 and 18 mM) using MTX-DODAB at a concentration of 2.91 mg/mL. It was observed that all these parameters affected the physiochemical characteristics of the produced liposomes. In this way, taking into account the size and PdI values of the obtained liposomal formulations it was established the agitation speed at 500 rpm, the use of a magnetic stirring bar with specific size and a DOPE concentration of 9 mM. Additionally, two different aqueous solutions were tested (water and PBS), however, it was observed that the use of PBS resulted in liposomal formulations with higher size and PdI values (data not shown). A possible explanation is the dissociation of the MTX-DODAB complex due to the interaction with the salts of the PBS and the fact that the free DODAB can induce a destabilization of the liposomes. Using these optimized conditions further optimizations were performed, relatively to the initial volume of water/ethanol (4 mL/4 mL versus 6 mL/6 mL) and the initial concentration of MTX-DODAB (2.18; 2.91 and 4.37 mg/mL). Table 7 shows the results obtained for these different conditions tested.

Table 7 | Characterization of the liposomal formulations obtained after several optimizations. Values are the mean ± SD of 2 independent experiments

Samples	Water/ ethanol volume (mL)	Z-average (nm)	PdI	Initial MTX (mg/mL)	Final MTX* (mg/mL)	EE (%)	Stability (weeks)
1	4/4	100.2 ± 0.2	0.049 ± 0.011	2.91	2.06 ± 0.08	70.8 ± 2.6	> 16
2	6/6	121.0 ± 3.6	0.055 ± 0.008	2.91	2.26 ± 0.06	77.5 ± 2.0	> 16
3	4/4	217.6 ± 0.6	0.132 ± 0.014	4.37	3.52 ± 0.15	80.6 ± 3.4	> 16
4	4/4	100.3 ± 0.9	0.055 ± 0.018	2.18	1.58 ± 0.07	72.3 ± 3.0	> 16
5	6/6	109.8 ± 0.4	0.066 ± 0.018	2.18	1.66 ± 0.14	76.4 ± 6.7	< 12

***Free MTX concentration was quantified by absorbance at 303 nm and then the final MTX concentration was calculated

The results obtained from the last optimizations (table 7) showed that the samples 1, 2, 4 and 5 revealed very similar size and PdI values. Sample 3, in which was tested a higher initial concentration of MTX-DODAB, revealed bigger values of size and PdI. Therefore, it can be inferred that the presence of a higher MTX-DODAB concentration can induce a destabilization in the liposomes formation, resulting in a more heterogeneous population of larger liposomes. Comparing the samples 1 and 2, which were produced using the same conditions with the exception of the water/ethanol volume, it was observed that sample 2 prepared using a higher volume of water/ethanol resulted in a higher EE of MTX. The same behavior was observed for the samples 4 and 5, where it was tested a lower concentration of MTX-DODAB (2.18 mg/mL). In this way, taking into account the final MTX concentration in the formulations as well as their stability along the time, sample 2 was selected for the next steps. This liposomal formulation demonstrated to be a monodispersed population of small and stealth liposomes with a high EE and stability during the storage, which are suitable characteristics for an IV therapeutic application.

In order to produce liposomes with targeting ability, the next step was the incorporation of a peptide containing FA in the chosen formulation. FA, as a targeting agent for drug delivery, presents several advantages in addition to its high affinity for the FR, such as low MW, easy chemical conjugation, lack of immunogenicity, water solubility and stability to diverse solvents, pH and temperature [88]. Moreover, FA is a widely used targeting approach in cancer because its receptor is overexpressed in cancer cells while its expression in healthy cells and organs is extremely limited [171]. In this

work it was used the targeting ligand FA linked to a peptide [166]. This conjugate inserts deeply into the lipid bilayer with high stability, resulting in the FA part located in the membrane surface, while the peptide is inserted into the lipid bilayer interior [166].

The physicochemical characterization of the empty liposomes and liposomes loaded with MTX-DODAB containing or not the FA-peptide was performed using DLS and NTA (table 8). All formulations revealed low PdI values (< 0.1), small size and high stability along time (> 16 weeks). Also, all developed formulations presented a zeta-potential close to zero (0 ± 3 mV), therefore these NPs have neutral charge. Furthermore, the NTA results corroborate the data obtained by DLS analysis. The concentration of particles, which was obtained by NTA, indicated a large number of particles in solution, increasing the probability of success of these formulations.

Table 8 | Physicochemical characterization of the optimal liposomal formulations evaluated by DLS and NTA. Values are the mean ± SD of 3 independent experiments

Formulations	DLS			NTA	
	Z-average (d.nm)	PdI	Stability (weeks)	Mean (d.nm)	Concentration (E^{13} particles/mL)
Liposomes	154.3 ± 1.4	0.072 ± 0.009	> 16	151.8 ± 6.3	2.26 ± 0.18
FA-Liposomes	147.0 ± 1.8	0.060 ± 0.009	> 16	142.0 ± 2.0	1.61 ± 0.24
Liposomes + MTX-DODAB	124.2 ± 0.7	0.046 ± 0.015	> 16	136.0 ± 7.4	3.95 ± 0.46
FA-Liposomes + MTX-DODAB	149.0 ± 1.2	0.090 ± 0.008	> 16	169.5 ± 3.4	2.57 ± 0.25

Figure 30 A, B, C and D shows the size distribution of liposomes, FA-liposomes, liposomes loaded with MTX-DODAB and FA-liposomes loaded with MTX-DODAB obtained by NTA, respectively. These distributions corroborate all the results obtained, indicating that these formulations are homogeneous populations with small liposomes.

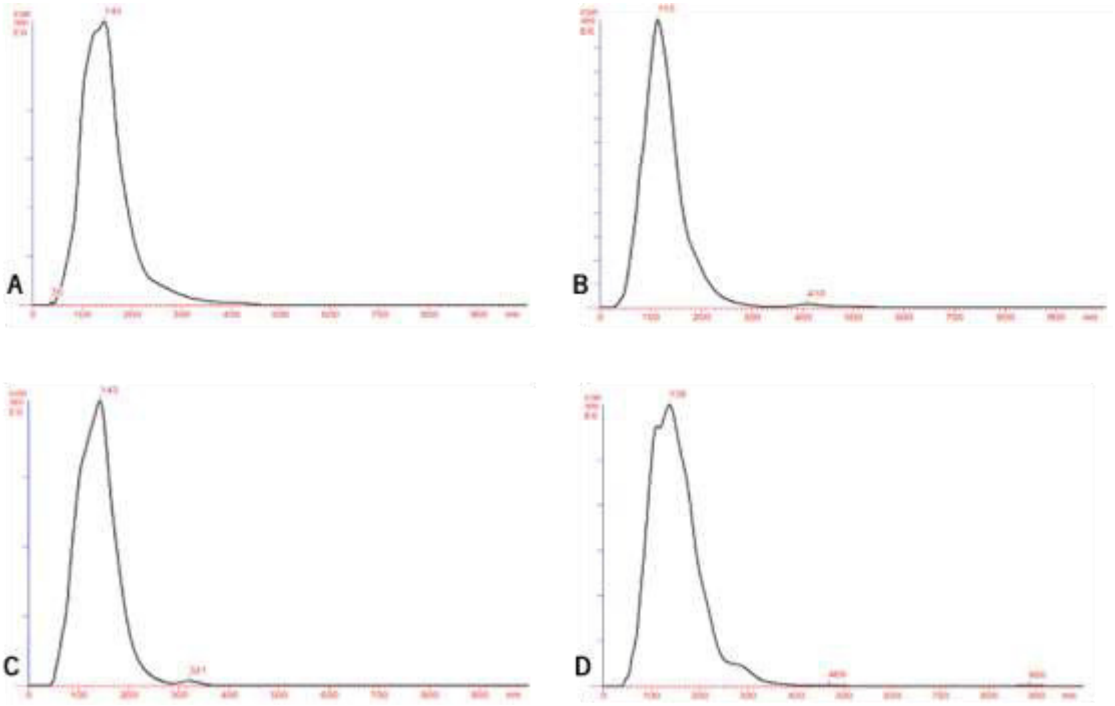

Figure 30 | Size distribution of the optimal liposomal formulations obtained by NTA. A) Liposomes; B) Liposomes + MTX-DODAB; C) FA-liposomes and D) FA-liposomes + MTX-DODAB.

Another important parameter in liposomes characterization, the concentration of MTX encapsulated in the liposomes containing or not FA at the surface, was determined by two different methods, ^{1}H NMR spectroscopy and absorbance method. The results demonstrated a great discrepancy between the values of encapsulated MTX obtained by the two methods (table 9).

Table 9 | Concentrations of MTX and its EE in liposomes containing or not FA at the surface determined by ^{1}H NMR and absorbance at 303 nm. Values are the mean ± SD of 3 independent experiments

Formulations	Initial MTX (mg/mL)	Final MTX (mg/mL) Absorbance (303 nm)	Final MTX (mg/mL) ^{1}H NMR	EE* (%)
Liposomes + MTX-DODAB	2.91	2.11 ± 0.13	0.44 ± 0.03	15.1 ± 1.0
FA-Liposomes + MTX-DODAB	2.91	2.05 ± 0.10	0.46 ± 0.03	16.0 ± 1.2

*EE was calculated taking into account the MTX concentration values obtained by ^{1}H NMR

The MTX quantification through ^{1}H NMR was performed in a direct way, in which the MTX was quantified by the liposomes analysis. On the other hand, using the absorbance method the

concentration of the encapsulated MTX was calculated after the quantification of free MTX (indirect method). This indirect method can induce more errors associated with the quantification of the encapsulated MTX. In this way, for further assays were taking into account the concentrations of MTX determined by ^{1}H NMR.

3.3. Evaluation of the biological effect of liposomes loaded with MTX-DODAB

The biological effect of the liposomes loaded with MTX-DODAB was evaluated using the Caco-2 cancer cell line. The cell viability of Caco-2 cells incubated with these liposomes and respective empty liposomes and free MTX (complexed with DODAB or not) was assessed by MTS assay. The results obtained can be visualized below in figure 31.

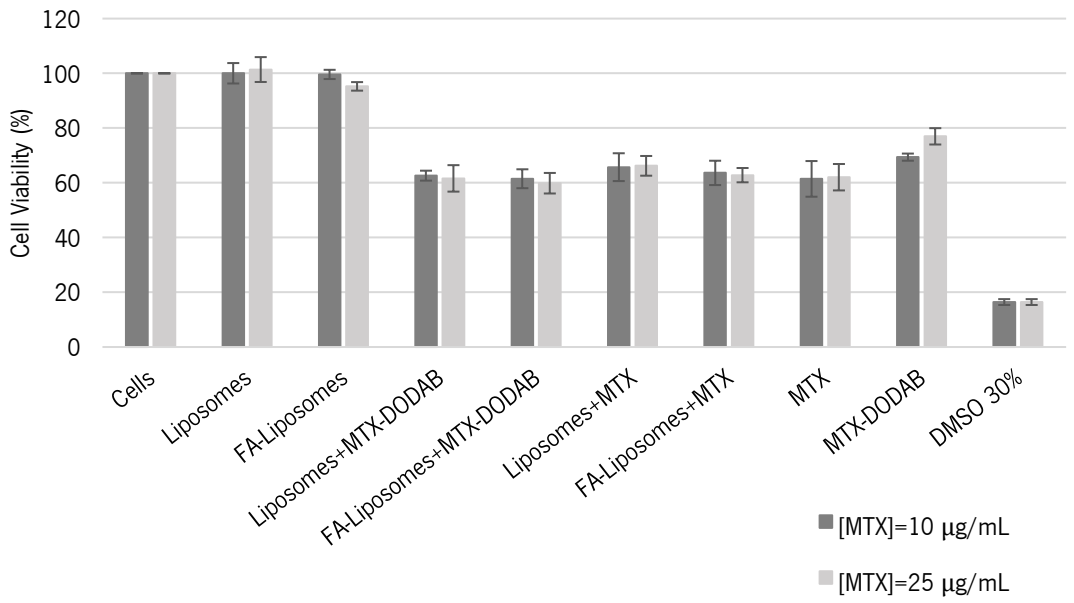

Figure 31 | Caco-2 cell line viability after 72 hours of contact with liposomes and free MTX, compared with cells (negative control) and cells incubated with 30 % of DMSO (death control), determined by MTS assay. Values are the mean ± SD of 3 independent experiments. The concentrations tested were 10 and 25 μg/mL.

Figure 31 shows that the liposomes containing or not FA loaded with MTX-DODAB and free MTX revealed very similar values of cell viability. A control using liposomes loaded with unmodified MTX was performed and it was observed that the cell viability is very similar to the liposomes loaded with MTX-DODAB. As expected, the empty liposomes did not induce cytotoxicity in Caco-2 cells. Also, cells incubated with MTX-DODAB demonstrated a slightly higher cell viability compared to cells incubated with MTX. A possible explanation is that the MTX-DODAB as a hydrophobic

derivative of MTX can precipitate in the presence of an aqueous medium (culture medium), reducing the MTX concentration that can interact with the cells, thus affecting the biological effect of the drug.

Cells incubated with FA-liposomes and non-targeted liposomes loaded with MTX-DODAB showed very similar cell viability values. Since DODAB is a lipid, it can be integrated into the bilayer of the liposomes, therefore the MTX complexed with this lipid can stay located on the outside of the liposomes. As MTX displays a similar chemical structure to FA [172-175], this drug is able to bind to FR and stop the pathways of *de novo* nucleotide synthesis, inducing cell death [172, 174]. Consequently, in addition to MTX presenting a great potential as a chemotherapeutic drug, it also appears to be a promising targeting ligand for cancer therapy [172, 175, 176]. This could explain the fact that the cells incubated with these formulations present very similar cell viability values, contrary to what is expected. Moreover, the liposomes were placed directly over the cells, which can induce their internalization through different ways and not only by the receptor-mediated endocytosis.

4. CONCLUSIONS

First of all, in this chapter it was successfully produced a hydrophobic MTX derivative (MTX-DODAB complex), using a green method. Then, several optimizations were performed for the production of liposomes loaded with MTX-DODAB by ethanol injection. The ideal formulation was reached using a DOPE concentration of 9 mM, water as aqueous phase, a MTX-DODAB concentration of 2.91 mg/mL and an initial water/ethanol volume of 6/6 mL. The obtained liposomes showed suitable characteristics for IV therapeutic applications (monodisperse population (PdI< 0.1) of small particles with neutral charge).

Additionally, the FA-peptide was added to the best liposomal formulation, in order to provide a specific targeting approach. It was observed that these FA-tagged liposomes also presented suitable characteristics for the intended purpose. The evaluation of the biological effect of the liposomes loaded with MTX-DODAB demonstrated a significant cytotoxicity against cancer cells, similar to free MTX.

In conclusion, with this work it was achieved the production of FA-tagged liposomes loaded with MTX-DODAB, which showed suitable characteristics for IV application in cancer therapy. In the future, it is expected to perform *in vivo* experiments using these promising liposomal formulations. Additionally, it can be tested the encapsulation of other MTX derivatives or other pharmacological compounds, for several other therapeutic purposes.

CHAPTER V

Conclusions

Chapter V – CONCLUSIONS

1. FINAL REMARKS

With this master thesis it was achieved the production of two types of PEGylated NPs (PTS micelles and liposomes) for the delivery of hydrophobic MTX derivatives, as intended. Both hydrophobic MTX derivatives (MTX-OEt and MTX-DODAB) were successfully produced in our laboratory and their characterization revealed the expected structure and their purity. PEGylated micelles were produced using PTS, also produced in our laboratory, which demonstrated a similar structure to the commercial one. After several optimizations, a homogeneous population of small and stealth micelles loaded with MTX-OEt was obtained using the auxiliary solvent method with evaporation at 30 °C, a PTS concentration of 15 mg/mL and a PTS/MTX-OEt mass ratio of 8:1. Liposomes with suitable characteristics were produced by ethanol injection using a DOPE concentration of 9 mM, water as aqueous phase, an MTX-DODAB concentration of 2.91 mg/mL and an initial water/ethanol volume of 6/6 mL.

PTS micelles loaded with MTX-OEt and liposomes loaded with MTX-DODAB demonstrated the expected biological effect against cancer cells (Caco-2 cell line), which was very similar to the biological effect of free MTX. These results indicated that these micelles possess the important ability to release the drugs and the MTX derivatives are promising prodrugs that can be used in cancer therapy.

2. FUTURE PERSPECTIVES

This master thesis showed promising results for both developed NPs (PTS micelles and liposomes), which revealed a great potential as DDS in cancer therapy. Therefore, additional research is needed for the development of more efficient DDS and for a better understanding of their biological effects. In the case of micelles, there is the need to incorporate a targeting agent, enabling a specific drug delivery. The developed liposomes already have a targeting agent, however, another important adjustment could be the introduction of alternative targeting agents. For both optimized NPs additional studies can be made such as *in vivo* experiments and testing their application in other relevant diseases, such as rheumatoid arthritis that is characterized by the presence of cells expressing the FR.

References

1. Sahoo, S.K., S. Parveen, and J.J. Panda, *The present and future of nanotechnology in human health care.* Nanomedicine: Nanotechnology, Biology and Medicine, 2007. **3**(1): p. 20-31.

2. Loureiro, A., *et al.*, *Albumin-Based Nanodevices as Drug Carriers.* Current Pharmaceutical Design, 2016. **22**(10): p. 1371-1390.

3. Farokhzad, O.C. and R. Langer, *Impact of Nanotechnology on Drug Delivery.* ACS Nano, 2009. **3**(1): p. 16-20.

4. Sanchez, F. and K. Sobolev, *Nanotechnology in concrete – A review.* Construction and Building Materials, 2010. **24**(11): p. 2060-2071.

5. Singh, R., S. Tiwari, and J. Tawaniya, *Review on nanotechnology with several aspects.* International Journal Of Research In Computer Engineering And Electronics, 2013. **2**(3): p. 1-8.

6. Lohcharoenkal, W., *et al.*, *Protein Nanoparticles as Drug Delivery Carriers for Cancer Therapy.* BioMed Research International, 2014. **2014**: p. 1-12.

7. Park, K., *Nanotechnology: What it can do for drug delivery.* Journal of Controlled Release, 2007. **120**(1-2): p. 1-3.

8. Liu, Y., H. Miyoshi, and M. Nakamura, *Nanomedicine for drug delivery and imaging: A promising avenue for cancer therapy and diagnosis using targeted functional nanoparticles.* International Journal of Cancer, 2007. **120**(12): p. 2527-2537.

9. Rizzo, L.Y., *et al.*, *Recent progress in nanomedicine: therapeutic, diagnostic and theranostic applications.* Current Opinion in Biotechnology, 2013. **24**(6): p. 1159-1166.

10. Mahapatro, A. and D.K. Singh, *Biodegradable nanoparticles are excellent vehicle for site directed in-vivo delivery of drugs and vaccines.* Journal of Nanobiotechnology, 2011. **9**(55): p. 1-11.

11. Ravichandran, R., *Nanotechnology-Based Drug Delivery Systems.* NanoBiotechnology, 2009. **5**(1): p. 17-33.

12. Suri, S.S., H. Fenniri, and B. Singh, *Nanotechnology-based drug delivery systems.* Journal of Occupational Medicine and Toxicology, 2007. **2**(16): p. 1-6.

13. Koo, O.M., I. Rubinstein, and H. Onyuksel, *Role of nanotechnology in targeted drug delivery and imaging: a concise review.* Nanomedicine: Nanotechnology, Biology and Medicine, 2005. **1**(3): p. 193-212.

14. Demetzos, C. and N. Pippa, *Advanced drug delivery nanosystems (aDDnSs): a mini-review.* Drug Delivery, 2014. **21**(4): p. 250-257.

15. Singh, R. and J.W. Lillard, *Nanoparticle-based targeted drug delivery.* Experimental and Molecular Pathology, 2009. **86**(3): p. 215-223.

16. Mignani, S., *et al.*, *Expand classical drug administration ways by emerging routes using dendrimer drug delivery systems: A concise overview.* Advanced Drug Delivery Reviews, 2013. **65**(10): p. 1316-1330.

17. Bose, T., *et al.*, *Overview of nano-drugs characteristics for clinical application: the journey from the entry to the exit point.* Journal of Nanoparticle Research, 2014. **16**(8): p. 1-25.

18. MaHam, A., *et al.*, *Protein-Based Nanomedicine Platforms for Drug Delivery.* Small, 2009. **5**(15): p. 1706-1721.

19. Couvreur, P. and C. Vauthier, *Nanotechnology: Intelligent Design to Treat Complex Disease.* Pharmaceutical Research, 2006. **23**(7): p. 1417-1450.

20. Shimanovich, U., *et al.*, *Protein micro- and nano-capsules for biomedical applications.* Chemical Society Reviews, 2014. **43**(5): p. 1361-1371.

21. Nikalje, A.P., *Nanotechnology and its Applications in Medicine.* Medicinal chemistry, 2015. **5**(2): p. 81-89.

22. Estanqueiro, M., *et al.*, *Nanotechnological carriers for cancer chemotherapy: The state of the art.* Colloids and Surfaces B: Biointerfaces, 2015. **126**: p. 631-648.

23. Rabanel, J.M., *et al.*, *Drug-Loaded Nanocarriers: Passive Targeting and Crossing of Biological Barriers.* Current Medicinal Chemistry, 2012. **19**(19): p. 3070-3102.

24. Yalkowsky, S.H., J.F. Krzyzaniak, and G.H. Ward, *Formulation-Related Problems Associated with Intravenous Drug Delivery.* Journal of Pharmaceutical Sciences, 1998. **87**(7): p. 787-796.

25. Blanco, E., H. Shen, and M. Ferrari, *Principles of nanoparticle design for overcoming biological barriers to drug delivery.* Nature Biotechnology, 2015. **33**(9): p. 941-951.

26. Wang, J., *et al.*, *More Effective Nanomedicines through Particle Design.* Small, 2011. **7**(14): p. 1919-1931.

27. Yona, S. and S. Gordon, *From the Reticuloendothelial to Mononuclear Phagocyte System – The Unaccounted Years.* Frontiers in Immunology, 2015. **6**: p. 1-7.

28. Owens, D.E. and N.A. Peppas, *Opsonization, biodistribution, and pharmacokinetics of polymeric nanoparticles.* International Journal of Pharmaceutics, 2006. **307**(1): p. 93-102.

29. Gatoo, M.A., *et al.*, *Physicochemical Properties of Nanomaterials: Implication in Associated Toxic Manifestations.* BioMed Research International, 2014. **2014**: p. 1-8.

30. Sun, T., *et al.*, *Engineered Nanoparticles for Drug Delivery in Cancer Therapy.* Angewandte Chemie International Edition, 2014. **53**(46): p. 12320-12364.

31. Desai, N., *Challenges in Development of Nanoparticle-Based Therapeutics.* The American Association of Pharmaceutical Scientists Journal, 2012. **14**(2): p. 282-295.

32. Riehemann, K., *et al.*, *Nanomedicine—Challenge and Perspectives.* Angewandte Chemie International Edition, 2009. **48**(5): p. 872-897.

33. Sanvicens, N. and M.P. Marco, *Multifunctional nanoparticles- properties and prospects for their use in human medicine.* Trends in Biotechnology, 2008. **26**(8): p. 425-433.

34. Duan, X. and Y. Li, *Physicochemical Characteristics of Nanoparticles Affect Circulation, Biodistribution, Cellular Internalization, and Trafficking.* Small, 2013. **9**(9-10): p. 1521-1532.

35. Haley, B. and E. Frenkel, *Nanoparticles for drug delivery in cancer treatment.* Urologic Oncology: Seminars and Original Investigations, 2008. **26**(1): p. 57-64.

36. Wacker, M., *Nanocarriers for intravenous injection—The long hard road to the market.* International Journal of Pharmaceutics, 2013. **457**(1): p. 50-62.

37. Alexis, F., *et al.*, *Factors Affecting the Clearance and Biodistribution of Polymeric Nanoparticles.* Molecular Pharmaceutics, 2008. **5**(4): p. 505-515.

38. Beija, M., *et al.*, *Colloidal systems for drug delivery: from design to therapy.* Trends in Biotechnology, 2012. **30**(9): p. 485-496.

39. Lundqvist, M., *et al.*, *Nanoparticle size and surface properties determine the protein corona with possible implications for biological impacts.* Proceedings of the National Academy of Sciences, 2008. **105**(38): p. 14265–14270.

40. Davis, M.E., Z. Chen, and D.M. Shin, *Nanoparticle therapeutics: an emerging treatment modality for cancer.* Nature Reviews Drug Discovery, 2008. **7**: p. 771-782.

41. Swami, A., *et al.*, *Nanoparticles for Targeted and Temporally Controlled Drug Delivery*, in *Multifunctional Nanoparticles for Drug Delivery Applications: Imaging, Targeting, and Delivery*, S. Svenson and R.K. Prud'homme, Editors. 2012, Springer US: Boston, MA. p. 9-29.

42. Alexis, F., *et al.*, *Nanoparticle Technologies for Cancer Therapy*, in *Drug Delivery*, M. Schäfer-Korting, Editor. 2010, Springer Berlin Heidelberg: Berlin, Heidelberg. p. 55-86.

43. Suk, J.S., *et al.*, *PEGylation as a strategy for improving nanoparticle-based drug and gene delivery.* Advanced Drug Delivery Reviews, 2016. **99**(Part A): p. 28-51.

44. Veronese, F.M. and G. Pasut, *PEGylation, successful approach to drug delivery.* Drug Discovery Today, 2005. **10**(21): p. 1451-1458.

45. Jokerst, J.V., *et al.*, *Nanoparticle PEGylation for imaging and therapy.* Nanomedicine, 2011. **6**(4): p. 715-728.

46. Harris, J.M., N.E. Martin, and M. Modi, *Pegylation: A Novel Process for Modifying Pharmacokinetics.* Clinical Pharmacokinetics, 2001. **40**(7): p. 539-551.

47. Vonarbourg, A., *et al.*, *Parameters influencing the stealthiness of colloidal drug delivery systems.* Biomaterials, 2006. **27**(24): p. 4356-4373.

48. Mosqueira, V.C., *et al.*, *Biodistribution of long-circulating PEG-grafted nanocapsules in mice: effects of PEG chain length and density.* Pharmaceutical Research, 2001. **18**(10): p. 1411-1419.

49. Gref, R., *et al.*, *'Stealth' corona-core nanoparticles surface modified by polyethylene glycol (PEG): influences of the corona (PEG chain length and surface density) and of the core composition on phagocytic uptake and plasma protein adsorption.* Colloids and Surfaces B: Biointerfaces, 2000. **18**(3): p. 301-313.

50. Barreto, J.A., *et al.*, *Nanomaterials: Applications in Cancer Imaging and Therapy.* Advanced Materials, 2011. **23**(12): p. 18-40.

51. Cho, K., *et al.*, *Therapeutic Nanoparticles for Drug Delivery in Cancer.* Clinical Cancer Research, 2008. **14**(5): p. 1310-1316.

52. Mirza, A.Z. and F.A. Siddiqui, *Nanomedicine and drug delivery: a mini review.* International Nano Letters, 2014. **4**(1): p. 1-7.

53. Sanna, V., N. Pala, and M. Sechi, *Targeted therapy using nanotechnology: focus on cancer.* International Journal of Nanomedicine, 2014. **9**: p. 467-483.

54. Zhang, L., *et al.*, *Nanoparticles in Medicine: Therapeutic Applications and Developments.* Clinical Pharmacology & Therapeutics, 2008. **83**(5): p. 761-769.

55. Chow, E.K.-H. and D. Ho, *Cancer Nanomedicine: From Drug Delivery to Imaging.* Science Translational Medicine, 2013. **5**(216): p. 1-12.

56. Caban, S., *et al.*, *Nanosystems for drug delivery.* OA Drug Design & Delivery, 2014. **2**(1): p. 1-7.

57. Wang, A.Z., *et al.*, *Biofunctionalized Targeted Nanoparticles for Therapeutic Applications.* Expert opinion on biological therapy, 2008. **8**(8): p. 1063-1070.

58. Elzoghby, A.O., W.M. Samy, and N.A. Elgindy, *Albumin-based nanoparticles as potential controlled release drug delivery systems.* Journal of Controlled Release, 2012. **157**(2): p. 168-182.

59. Nagavarma, B.V.N., *et al.*, *Different techniques for preparation of polymeric nanoparticles-A review.* Asian Journal of Pharmaceutical and Clinical Research, 2012. **5**(3): p. 16-23.

60. Kulthe, S.S., *et al.*, *Polymeric micelles: authoritative aspects for drug delivery.* Designed Monomers and Polymers, 2012. **15**(5): p. 465-521.

61. Zhou, Q., *et al.*, *Stimuli-responsive polymeric micelles for drug delivery and cancer therapy.* International Journal of Nanomedicine, 2018. **13**: p. 2921-2942.

62. Yokoyama, M., *Polymeric micelles as a new drug carrier system and their required considerations for clinical trials.* Expert Opinion on Drug Delivery, 2010. **7**(2): p. 145-158.

63. Oerlemans, C., *et al.*, *Polymeric Micelles in Anticancer Therapy: Targeting, Imaging and Triggered Release.* Pharmaceutical Research, 2010. **27**(12): p. 2569-2589.

64. Kim, S., *et al.*, *Overcoming the barriers in micellar drug delivery: loading efficiency, in vivo stability, and micelle–cell interaction.* Expert Opinion on Drug Delivery, 2010. **7**(1): p. 49-62.

65. Zhang, Y., Y. Huang, and S. Li, *Polymeric Micelles: Nanocarriers for Cancer-Targeted Drug Delivery.* AAPS PharmSciTech, 2014. **15**(4): p. 862-871.

66. Jhaveri, A.M. and V.P. Torchilin, *Multifunctional polymeric micelles for delivery of drugs and siRNA.* Frontiers in Pharmacology, 2014. **5**(77): p. 1-26.

67. Lee, K.-Y., *et al.*, *Vitamin E containing polymer micelles for reducing normal cell cytotoxicity and enhancing chemotherapy efficacy.* Acta Biomaterialia, 2015. **24**: p. 286-296.

68. Lu, Y. and K. Park, *Polymeric Micelles and Alternative Nanonized Delivery Vehicles for Poorly Soluble Drugs.* International journal of pharmaceutics, 2013. **453**(1): p. 198-214.

69. Mohamed, S., *et al.*, *Polymeric nano-micelles: versatile platform for targeted delivery in cancer.* Therapeutic Delivery, 2014. **5**(10): p. 1101-1121.

70. Xu, W., P. Ling, and T. Zhang, *Polymeric Micelles, a Promising Drug Delivery System to Enhance Bioavailability of Poorly Water-Soluble Drugs.* Journal of Drug Delivery, 2013. **2013**: p. 1-15.

71. Gong, J., *et al.*, *Polymeric micelles drug delivery system in oncology.* Journal of Controlled Release, 2012. **159**(3): p. 312-323.

72. Duhem, N., F. Danhier, and V. Préat, *Vitamin E-based nanomedicines for anti-cancer drug delivery.* Journal of Controlled Release, 2014. **182**: p. 33-44.

73. Croy, S.R. and G.S. Kwon, *Polymeric Micelles for Drug Delivery.* Current Pharmaceutical Design, 2006. **12**(36): p. 4669-4684.

74. Ahmad, Z., *et al.*, *Polymeric micelles as drug delivery vehicles.* RSC Advances, 2014. **4**(33): p. 17028-17038.

75. Dominguez, A., *et al.*, *Determination of Critical Micelle Concentration of Some Surfactants by Three Techniques.* Journal of Chemical Education, 1997. **74**(10): p. 1227-1231.

76. Torchilin, V.P., *Lipid-Core Micelles for Targeted Drug Delivery.* Current Drug Delivery, 2005. **2**(4): p. 319-327.

77. Kedar, U., *et al.*, *Advances in polymeric micelles for drug delivery and tumor targeting.* Nanomedicine: Nanotechnology, Biology and Medicine, 2010. **6**(6): p. 714-729.

78. Shin, D.H., Y.T. Tam, and G.S. Kwon, *Polymeric micelle nanocarriers in cancer research.* Frontiers of Chemical Science and Engineering, 2016. **10**(3): p. 348-359.

79. Batrakova, E.V., *et al.*, *Polymer Micelles as Drug Carriers*, in *Nanoparticulates as Drug Carriers*. 2006. p. 57-93.

80. Aliabadi, H.M. and A. Lavasanifar, *Polymeric micelles for drug delivery.* Expert Opinion on Drug Delivery, 2006. **3**(1): p. 139-162.

81. Kaur, K., *et al.*, *Micelles drug delivery for poorly soluble drug: A review.* World Journal of Pharmacy and Pharmaceutical Sciences, 2016. **5**(4): p. 617-635.

82. Mittal, A. and D. Chitkara, *Structural modifications in polymeric micelles to impart multifunctionality for improved drug delivery.* Therapeutic Delivery, 2016. **7**(2): p. 73-87.

83. Fleige, E., M.A. Quadir, and R. Haag, *Stimuli-responsive polymeric nanocarriers for the controlled transport of active compounds: concepts and applications.* Advanced drug delivery reviews, 2012. **64**(9): p. 866-884.

84. Lu, J., *et al.*, *Design and Characterization of PEG-Derivatized Vitamin E as a Nanomicellar Formulation for Delivery of Paclitaxel.* Molecular Pharmaceutics, 2013. **10**(8): p. 2880-2890.

85. Li, Y., *et al.*, *Design and Validation of PEG-Derivatized Vitamin E Copolymer for Drug Delivery into Breast Cancer.* Bioconjugate Chemistry, 2016. **27**(8): p. 1889-1899.

86. Kalepu, S. and V. Nekkanti, *Insoluble drug delivery strategies: review of recent advances and business prospects.* Acta Pharmaceutica Sinica. B, 2015. **5**(5): p. 442-453.

87. Daraee, H., *et al.*, *Application of liposomes in medicine and drug delivery.* Artificial Cells, Nanomedicine, and Biotechnology, 2016. **44**(1): p. 381-391.

88. Nogueira, E., *et al.*, *Design of liposomal formulations for cell targeting.* Colloids and Surfaces B: Biointerfaces, 2015. **136**: p. 514-526.

89. Pandey, H., R. Rani, and V. Agarwal, *Liposome and Their Applications in Cancer Therapy.* Brazilian Archives of Biology and Technology, 2016. **59**: p. 1-10.

90. Laouini, A., *et al.*, *Preparation, Characterization and Applications of Liposomes: State of the Art.* Journal of Colloid Science and Biotechnology, 2012. **1**(2): p. 147-168.

91. Moussa, H.G., A.M. Martins, and G.A. Husseini, *Review on Triggered Liposomal Drug Delivery with a Focus on Ultrasound.* Current Cancer Drug Targets, 2015. **15**(4): p. 282-313.

92. Pattni, B.S., V.V. Chupin, and V.P. Torchilin, *New Developments in Liposomal Drug Delivery.* Chemical Reviews, 2015. **115**(19): p. 10938-10966.

93. Roberts, S.A. and N. Agrawal. *Enhancing the drug encapsulation efficiency of liposomes for therapeutic delivery*. in *2017 IEEE Healthcare Innovations and Point of Care Technologies (HI-POCT)*. 2017.

94. Meure, L.A., N.R. Foster, and F. Dehghani, *Conventional and Dense Gas Techniques for the Production of Liposomes: A Review.* AAPS PharmSciTech, 2008. **9**(3): p. 798-809.

95. Santo, I.E., *et al.*, *Liposomes Size Engineering by Combination of Ethanol Injection and Supercritical Processing.* Journal of Pharmaceutical Sciences, 2015. **104**(11): p. 3842-3850.

96. Swaminathan, J. and C. Ehrhardt, *Liposomes for Pulmonary Drug Delivery*, in *Controlled Pulmonary Drug Delivery*, H.D.C. Smyth and A.J. Hickey, Editors. 2011, Springer New York: New York, NY. p. 313-334.

97. Wagner, A. and K. Vorauer-Uhl, *Liposome Technology for Industrial Purposes.* Journal of Drug Delivery, 2011. **2011**: p. 1-9.

98. Sercombe, L., *et al.*, *Advances and Challenges of Liposome Assisted Drug Delivery.* Frontiers in Pharmacology, 2015. **6**(286): p. 1-13.

99. Patil, Y.P. and S. Jadhav, *Novel methods for liposome preparation.* Chemistry and Physics of Lipids, 2014. **177**: p. 8-18.

100. Bozzuto, G. and A. Molinari, *Liposomes as nanomedical devices.* International Journal of Nanomedicine, 2015. **10**: p. 975-999.

101. Akbarzadeh, A., *et al.*, *Liposome: classification, preparation, and applications.* Nanoscale Research Letters, 2013. **8**(1): p. 102-110.

102. Charcosset, C., *et al.*, *Preparation of liposomes at large scale using the ethanol injection method: Effect of scale-up and injection devices.* Chemical Engineering Research and Design, 2015. **94**: p. 508-515.

103. Sala, M., *et al.*, *Preparation of liposomes: A comparative study between the double solvent displacement and the conventional ethanol injection—From laboratory scale to large scale.* Colloids and Surfaces A: Physicochemical and Engineering Aspects, 2017. **524**(C): p. 71-78.

104. Sharma, S., *et al.*, *Liposomes: Vesicular system an overview.* International Journal of Pharmacy and Pharmaceutical Sciences 2010. **2**(4): p. 15-21.

105. Li, J., *et al.*, *A review on phospholipids and their main applications in drug delivery systems.* Asian Journal of Pharmaceutical Sciences, 2015. **10**(2): p. 81-98.

106. Yingchoncharoen, P., D.S. Kalinowski, and D.R. Richardson, *Lipid-Based Drug Delivery Systems in Cancer Therapy: What Is Available and What Is Yet to Come.* Pharmacological Reviews, 2016. **68**(3): p. 701-787.

107. Luo, D., K.A. Carter, and J.F. Lovell, *Nanomedical Engineering: shaping future nanomedicines.* Wiley interdisciplinary reviews: Nanomedicine and nanobiotechnology, 2015. **7**(2): p. 169-188.

108. Bulbake, U., *et al.*, *Liposomal Formulations in Clinical Use: An Updated Review.* Pharmaceutics, 2017. **9**(2): p. 12-44.

109. Immordino, M.L., F. Dosio, and L. Cattel, *Stealth liposomes: review of the basic science, rationale, and clinical applications, existing and potential.* International Journal of Nanomedicine, 2006. **1**(3): p. 297-315.

110. Das, M., C. Mohanty, and S.K. Sahoo, *Ligand-based targeted therapy for cancer tissue.* Expert Opinion on Drug Delivery, 2009. **6**(3): p. 285-304.

111. Wicki, A., *et al.*, *Nanomedicine in cancer therapy: Challenges, opportunities, and clinical applications.* Journal of Controlled Release, 2015. **200**: p. 138-157.

112. Jabir, N.R., *et al.*, *Nanotechnology-based approaches in anticancer research.* International Journal of Nanomedicine, 2012. **7**: p. 4391-4408.

113. Gu, F.X., *et al.*, *Targeted nanoparticles for cancer therapy.* Nano Today, 2007. **2**(3): p. 14-21.

114. Bharali, D.J. and S.A. Mousa, *Emerging nanomedicines for early cancer detection and improved treatment: Current perspective and future promise.* Pharmacology & Therapeutics, 2010. **128**(2): p. 324-335.

115. Peer, D., *et al.*, *Nanocarriers as an emerging platform for cancer therapy.* Nature Nanotechnology, 2007. **2**: p. 751-760.

116. Sinha, R., *et al.*, *Nanotechnology in cancer therapeutics: bioconjugated nanoparticles for drug delivery.* Molecular Cancer Therapeutics, 2006. **5**(8): p. 1909-1917.

117. Murthy, S.K., *Nanoparticles in modern medicine: State of the art and future challenges.* International Journal of Nanomedicine, 2007. **2**(2): p. 129-141.

118. Pathak, P. and V.K. Katiyar. *Multi-Functional Nanoparticles and Their Role in Cancer Drug Delivery – A Review*. 2007; Available from: https://www.azonano.com/article.aspx?ArticleID=1903.

119. Danhier, F., O. Feron, and V. Préat, *To exploit the tumor microenvironment: Passive and active tumor targeting of nanocarriers for anti-cancer drug delivery.* Journal of Controlled Release, 2010. **148**(2): p. 135-146.

120. Wang, E.C. and A.Z. Wang, *Nanoparticles and their applications in cell and molecular biology.* Integrative biology, 2014. **6**(1): p. 9-26.

121. Huynh, N.T., *et al.*, *The rise and rise of stealth nanocarriers for cancer therapy: passive versus active targeting.* Nanomedicine, 2010. **5**(9): p. 1415-1433.

122. Sahoo, S.K. and V. Labhasetwar, *Nanotech approaches to drug delivery and imaging.* Drug Discovery Today, 2003. **8**(24): p. 1112-1120.

123. Torchilin, V.P., *Passive and Active Drug Targeting: Drug Delivery to Tumors as an Example*, in *Drug Delivery*, M. Schäfer-Korting, Editor. 2010, Springer Berlin Heidelberg: Berlin, Heidelberg. p. 3-53.

124. Choi, C.H.J., *et al.*, *Mechanism of active targeting in solid tumors with transferrin-containing gold nanoparticles.* Proceedings of the National Academy of Sciences of the United States of America, 2010. **107**(3): p. 1235-1240.

125. Basile, L., R. Pignatello, and C. Passirani, *Active Targeting Strategies for Anticancer Drug Nanocarriers.* Current Drug Delivery, 2012. **9**(3): p. 255-268.

126. Krall, N., J. Scheuermann, and D. Neri, *Small Targeted Cytotoxics: Current State and Promises from DNA-Encoded Chemical Libraries.* Angewandte Chemie International Edition, 2013. **52**(5): p. 1384-1402.

127. Park, J.H., *et al.*, *Polymeric nanomedicine for cancer therapy.* Progress in Polymer Science, 2008. **33**(1): p. 113-137.

128. Teng, L., *et al.*, *Clinical translation of folate receptor-targeted therapeutics.* Expert Opinion on Drug Delivery, 2012. **9**(8): p. 901-908.

129. Yang, J., E. Vlashi, and P. Low, *Folate-Linked Drugs for the Treatment of Cancer and Inflammatory Diseases*, in *Water Soluble Vitamins: Clinical Research and Future Application*, O. Stanger, Editor. 2012, Springer Netherlands: Dordrecht. p. 163-179.

130. Yi, Y.-S., *Folate Receptor-Targeted Diagnostics and Therapeutics for Inflammatory Diseases.* Immune Network, 2016. **16**(6): p. 337-343.

131. Low, P.S. and S.A. Kularatne, *Folate-targeted therapeutic and imaging agents for cancer.* Current Opinion in Chemical Biology, 2009. **13**(3): p. 256-262.

132. Sudimack, J. and R.J. Lee, *Targeted drug delivery via the folate receptor.* Advanced Drug Delivery Reviews, 2000. **41**(2): p. 147-162.

133. Matsuoka, H., *et al.*, *Antirheumatic Agents: Novel Methotrexate Derivatives Bearing a Benzoxazine or Benzothiazine Moiety.* Journal of Medicinal Chemistry, 1997. **40**(1): p. 105-111.

134. Brown, P.M., A.G. Pratt, and J.D. Isaacs, *Mechanism of action of methotrexate in rheumatoid arthritis, and the search for biomarkers.* Nature Reviews Rheumatology, 2016. **12**: p. 731-742.

135. Blanco-Fernandez, B., *et al.*, *Dually sensitive dextran-based micelles for methotrexate delivery.* RSC Advances, 2017. **7**(24): p. 14448-14460.

136. Yousefi, G., *et al.*, *Synthesis and Characterization of Methotrexate Polyethylene Glycol Esters as a Drug Delivery System.* Chemical and Pharmaceutical Bulletin, 2010. **58**(2): p. 147-153.

137. Campbell, J.M., *et al.*, *Methotrexate-induced toxicity pharmacogenetics: an umbrella review of systematic reviews and meta-analyses.* Cancer Chemotherapy and Pharmacology, 2016. **78**(1): p. 27-39.

138. Ren, J., *et al.*, *A micelle-like structure of poloxamer–methotrexate conjugates as nanocarrier for methotrexate delivery.* International Journal of Pharmaceutics, 2015. **487**(1): p. 177-186.

139. Jeong, Y.-I., *et al.*, *Methotrexate-incorporated polymeric micelles composed of methoxy poly(ethylene glycol)-grafted chitosan.* Macromolecular Research, 2009. **17**(7): p. 538-543.

140. Bansal, D.B., *et al.*, *PEGylated methotrexate based micellar conjugates for anticancer chemotherapy.* Asian Journal of Pharmaceutics, 2015. **9**(1): p. 60-66.

141. Chabner, B.A. and T.G. Roberts Jr, *Chemotherapy and the war on cancer.* Nature Reviews Cancer, 2005. **5**: p. 65-72.

142. Pignatello, R., *et al.*, *Lipophilic methotrexate conjugates with antitumor activity.* European Journal of Pharmaceutical Sciences, 2000. **10**(3): p. 237-245.

143. Sikorska, M., *et al.*, *Nanomicellar formulation of coenzyme Q10 (Ubisol-Q10) effectively blocks ongoing neurodegeneration in the mouse 1-methyl-4-phenyl-1,2,3,6-*

tetrahydropyridine model: potential use as an adjuvant treatment in Parkinson's disease. Neurobiology of Aging, 2014. **35**(10): p. 2329-2346.

144. Borowy-Borowski, H., *et al.*, *Unique Technology for Solubilization and Delivery of Highly Lipophilic Bioactive Molecules.* Journal of Drug Targeting, 2004. **12**(7): p. 415-424.

145. Sikorska, M., *et al.*, *Derivatised α-tocopherol as a CoQ10 carrier in a novel water-soluble formulation.* Biofactors, 2003. **18**(1-4): p. 173-183.

146. Muddineti, O.S., B. Ghosh, and S. Biswas, *Current trends in the use of vitamin E-based micellar nanocarriers for anticancer drug delivery.* Expert Opinion on Drug Delivery, 2017. **14**(6): p. 715-726.

147. ATCC. *BJ-5ta (ATCC® CRL-4001™)*. 2016; Available from: https://www.lgcstandards-atcc.org/products/all/CRL-4001.aspx#characteristics.

148. ATCC. *Caco-2 [Caco2] (ATCC® HTB-37™)*. 2016; Available from: https://www.lgcstandards-atcc.org/Products/All/HTB-37.aspx?geo_country=pt.

149. Promega. *CellTiter 96® AQueous One Solution Cell Proliferation Assay (MTS)*. 2018; Available from: https://worldwide.promega.com/products/cell-health-assays/cell-viability-and-cytotoxicity-assays/celltiter-96-aqueous-one-solution-cell-proliferation-assay-_mts_/?catNum=G3582.

150. Malich, G., B. Markovic, and C. Winder, *The sensitivity and specificity of the MTS tetrazolium assay for detecting the in vitro cytotoxicity of 20 chemicals using human cell lines.* Toxicology, 1997. **124**(3): p. 179-192.

151. Kolate, A., *et al.*, *PEG — A versatile conjugating ligand for drugs and drug delivery systems.* Journal of Controlled Release, 2014. **192**: p. 67-81.

152. Danaei, M., *et al.*, *Impact of Particle Size and Polydispersity Index on the Clinical Applications of Lipidic Nanocarrier Systems.* Pharmaceutics, 2018. **10**(2): p. 57-73.

153. Dhand, C., *et al.*, *Role of size of drug delivery carriers for pulmonary and intravenous administration with emphasis on cancer therapeutics and lung-targeted drug delivery.* RSC Advances, 2014. **4**(62): p. 32673-32689.

154. Gaumet, M., *et al.*, *Nanoparticles for drug delivery: The need for precision in reporting particle size parameters.* European Journal of Pharmaceutics and Biopharmaceutics, 2008. **69**(1): p. 1-9.

155. Lipshutz, B.H. and A.R. Abela, *Micellar Catalysis of Suzuki–Miyaura Cross-Couplings with Heteroaromatics in Water.* Organic Letters, 2008. **10**(23): p. 5329-5332.

156. Clogston, J.D. and A.K. Patri, *Zeta Potential Measurement*, in *Characterization of Nanoparticles Intended for Drug Delivery*, S.E. McNeil, Editor. 2011, Humana Press: Totowa, NJ. p. 63-70.

157. Lewinski, N., V. Colvin, and R. Drezek, *Cytotoxicity of Nanoparticles.* Small, 2008. **4**(1): p. 26-49.

158. Kong, B., *et al.*, *Experimental considerations on the cytotoxicity of nanoparticles.* Nanomedicine (London, England), 2011. **6**(5): p. 929-941.

159. Li, W., J. Zhou, and Y. Xu, *Study of the in vitro cytotoxicity testing of medical devices.* Biomedical Reports, 2015. **3**(5): p. 617-620.

160. Lamch, Ł., *et al.*, *Polymeric micelles for enhanced Photofrin II® delivery, cytotoxicity and pro-apoptotic activity in human breast and ovarian cancer cells.* Photodiagnosis and Photodynamic Therapy, 2014. **11**(4): p. 570-585.

161. Behera, A.L., *et al.*, *Nanosizing of drugs: A promising approach for drug delivery.* Der Pharmacia Sinica, 2010. **1**(1): p. 20-28.

162. Shahed-Al-Mahmud, M. and E.H. Bhuiuan, *Nanoparticles Using as Efficient Bioavailability in Drug Delivery System- Mini Review.* Modern Applications of Bioequivalence and Bioavailability, 2018. **3**(1): p. 1-4.

163. Li, Z., *et al.*, *Cancer drug delivery in the nano era: An overview and perspectives.* Oncology Reports, 2017. **38**(2): p. 611-624.

164. Nogueira, E., *et al.*, *Neutral PEGylated liposomal formulation for efficient folate-mediated delivery of MCL1 siRNA to activated macrophages.* Colloids and Surfaces B: Biointerfaces, 2017. **155**: p. 459-465.

165. Nogueira, E., *et al.*, *Enhancing Methotrexate Tolerance with Folate Tagged Liposomes in Arthritic Mice.* Journal of Biomedical Nanotechnology, 2015. **11**(12): p. 2243-2252.

166. Nogueira, E., *et al.*, *Peptide Anchor for Folate-Targeted Liposomal Delivery.* Biomacromolecules, 2015. **16**(9): p. 2904-2910.

167. Ohradanova-Repic, A., *et al.*, *Fab antibody fragment-functionalized liposomes for specific targeting of antigen-positive cells.* Nanomedicine: Nanotechnology, Biology and Medicine, 2018. **14**(1): p. 123-130.

168. Della Porta, G., R. Campardelli, and E. Reverchon, *Monodisperse biopolymer nanoparticles by Continuous Supercritical Emulsion Extraction.* The Journal of Supercritical Fluids, 2013. **76**: p. 67-73.

169. Coimbra, M., *et al.*, *Improving solubility and chemical stability of natural compounds for medicinal use by incorporation into liposomes.* International Journal of Pharmaceutics, 2011. **416**(2): p. 433-442.

170. Petros, R.A. and J.M. DeSimone, *Strategies in the design of nanoparticles for therapeutic applications.* Nature Reviews Drug Discovery, 2010. **9**(2010): p. 615–627.

171. Zwicke, G.L., G.A. Mansoori, and C.J. Jeffery, *Utilizing the folate receptor for active targeting of cancer nanotherapeutics.* Nano Reviews, 2012. **3**: p. 18496-18506.

172. Chen, Y., *et al.*, *The therapeutic effect of methotrexate-conjugated Pluronic-based polymeric micelles on the folate receptor-rich tumors treatment.* International Journal of Nanomedicine, 2015. **10**: p. 4043-4057.

173. Thomas, T.P., *et al.*, *Design and In vitro Validation of Multivalent Dendrimer Methotrexates as a Folate-targeting Anticancer Therapeutic.* Current pharmaceutical design, 2013. **19**(37): p. 6594-6605.

174. Lima, A., *et al.*, *Genetic polymorphisms in low-dose methotrexate transporters: current relevance as methotrexate therapeutic outcome biomarkers.* Pharmacogenomics, 2014. **15**(12): p. 1611-1635.

175. Rosenholm, J.M., *et al.*, *Cancer-Cell-Specific Induction of Apoptosis Using Mesoporous Silica Nanoparticles as Drug-Delivery Vectors.* Small, 2010. **6**(11): p. 1234-1241.

176. Wong, P.T. and S.K. Choi, *Mechanisms and Implications of Dual-Acting Methotrexate in Folate-Targeted Nanotherapeutic Delivery.* International Journal of Molecular Sciences, 2015. **16**(1): p. 1772-1790.